



**Calhoun: The NPS Institutional Archive**  
**DSpace Repository**

---

NPS Scholarship

Theses

---

1969

A study of radar pulse compression using complementary series to modulate the transmitted waveform.

Sieren, Gerald Joseph

Monterey, California. U.S. Naval Postgraduate School

---

<https://hdl.handle.net/10945/13179>

---

*Downloaded from NPS Archive: Calhoun*



Calhoun is the Naval Postgraduate School's public access digital repository for research materials and institutional publications created by the NPS community. Calhoun is named for Professor of Mathematics Guy K. Calhoun, NPS's first appointed -- and published -- scholarly author.

**Dudley Knox Library / Naval Postgraduate School**  
**411 Dyer Road / 1 University Circle**  
**Monterey, California USA 93943**

<http://www.nps.edu/library>

**NPS ARCHIVE**  
**1969**  
**SIEREN, G.**

A STUDY OF RADAR PULSE COMPRESSION  
USING COMPLEMENTARY SERIES TO  
MODULATE THE TRANSMITTED WAVEFORM

Gerald Joseph Sieren



# United States Naval Postgraduate School



## THE SIS

A STUDY OF RADAR PULSE COMPRESSION  
USING COMPLEMENTARY SERIES TO  
MODULATE THE TRANSMITTED WAVEFORM

by

Gerald J. Sieren

December 1969

*This document has been approved for public re-  
lease and sale; its distribution is unlimited.*

T133793

LIBRARY  
NAVAL POSTGRADUATE SCHOOL  
MONTEREY, CALIF. 93940

A STUDY OF RADAR PULSE COMPRESSION  
USING COMPLEMENTARY SERIES TO  
MODULATE THE TRANSMITTED WAVEFORM

by

Gerald Joseph Sieren  
Lieutenant, United States Navy  
B.S., University of Kansas, 1964

Submitted in partial fulfillment of the  
requirements for the degree of  
MASTER OF SCIENCE IN ELECTRICAL ENGINEERING

from the

NAVAL POSTGRADUATE SCHOOL  
December 1969

1969

SIEREN, G.

## ABSTRACT

Pulse compression radars have resulted from the need to put more energy into a transmitted pulse by increasing the pulse duration, yet retaining or improving the target range resolution. FM chirp and phase-coded pulse compression using a single binary code to modulate the carrier are somewhat degraded by the amount of hash, or range sidelobes in the output of the matched-filter receiver.

Pulse compression using complementary series, in which two binary series are transmitted, results in no range sidelobes in the detected pulse, since the autocorrelation functions of the two series completely cancel each other everywhere except at zero shift, where they add to produce a sharp peak with amplitude  $2N$  times the received pulse amplitude, where  $N$  is the number of digits in each series.

After introductory material on complementary series and pulse-compression systems, this thesis discusses the design, construction and testing of a pulse-compression system using complementary series of length four. The intent was to show feasibility, rather than to produce results using actual targets.

TABLE OF CONTENTS

CHAPTER	PAGE
I. INTRODUCTION -----	7
II. PULSE COMPRESSION RADARS -----	13
III. COMPLEMENTARY SERIES -----	22
IV. DESIGN EXAMPLE OF AN AUTOCORRELATION FUNCTION PULSE-COMPRESSION RADAR USING COMPLEMENTARY SERIES OF LENGTH FOUR.	
A. GENERATION OF PHASE-CODED PULSES -----	28
B. PROPOSAL USING A SINGLE DELAY LINE TO BOTH GENERATE AND RECEIVE THE PULSES -----	32
C. PROPOSALS USING SEPARATE DELAY LINES TO GENERATE AND AUTOCORRELATE PULSES -----	36
D. FINAL CONFIGURATION OF THE SYSTEM BUILT -----	46
E. MTI COMPATIBILITY -----	52
V. SUMMARY AND CONCLUSIONS	
A. SUMMARY -----	59
B. AREAS FOR POTENTIAL STUDY -----	60
APPENDIX A. DELAY LINE CHARACTERISTICS -----	62
APPENDIX B. TRANSMIT-RECEIVE SWITCH -----	65
APPENDIX C. SCALING ADDERS -----	66
APPENDIX D. CIRCUIT DIAGRAM OF THE MODULATOR USED TO REPLACE THE DELAY LINE FOR GENERATING THE TRANSMITTED PULSES -----	67
APPENDIX E. BUFFING AMPLIFIERS -----	68
APPENDIX F. PHASE INVERTERS -----	69



CHAPTER

PAGE

APPENDIX G. GATED AMPLIFIER ----- 70

APPENDIX H. RELCOM PHASE DETECTORS ----- 71

REFERENCES ----- 72

## LIST OF ILLUSTRATIONS

FIGURE	PAGE
2.1 Frequency modulation of the chirp radar -----	14
2.2 Autocorrelation of the binary Barker series of length five -----	17
2.3 List of all known binary Barker codes -----	19
3.1 Autocorrelation of a complementary series of length four -----	25
4.1 Phase-reversal modulation using the five- digit binary Barker code -----	29
4.2 RF pulse generated on a tapped delay line using a four-digit binary Barker code -----	30
4.3 Single delay line pulse generator-auto- correlator -----	34
4.4 Laboratory model of the system of Fig. 4.3 -----	35
4.5 Pulse compression using separate delay lines to generate and autocorrelate waveforms -----	37
4.6 Laboratory version of the system of Fig. 4.5 ---	38
4.7 Output of the system in Figure 4.6 -----	41
4.8 System as in Figure 4.6, but arranged to phase detect before autocorrelation -----	43
4.9 Output of the system in Figure 4.8 -----	44
4.10 Output of the system in Figure 4.8, but arranged to generate and autocorrelate the second member of the complementary pair -----	45

FIGURE	PAGE	
4.11	Final configuration of the pulse generator of the system built -----	47
4.12	Final configuration of the matched-filter receiver of the system built -----	48
4.13	Output of the system of Fig. 4.12 -----	49
4.14	Photograph illustrating sidelobe cancellation--	50
4.15	Output characteristics of the Relcom M1 phase detector -----	50
4.16	MTI radar -----	53
4.17	Illustration of the MTI "butterfly" effect ----	56
4.18	Video pulse trains of the MTI radar -----	57
A.1	Lumped-parameter delay line -----	63
B.1	Transmit-receive switch -----	65
C.1	RCA CA-3029A operational amplifier used as a scaling adder -----	66
D.1	Modulator for generating the transmitted waveform -----	67
E.1	Buffer amplifier -----	68
F.1	Phase inverter used for phase-reversal modulation -----	69
G.1	Gated amplifier -----	70
H.1	Schematic of the Relcom M1 phase detector -----	71

## I. INTRODUCTION

The function of most radar systems is the detection, location and possibly the tracking of targets. In addition, it is usually desirable to obtain target velocity information, and in many cases an MTI, or Moving Target Indication, capability is necessary.

Modern search radars are required to obtain targets at greater and greater ranges. One approach to the problem of increasing the range capability of a radar is to examine the constraints imposed by the radar range equation and consider those parameters which are under the control of the designer, especially those which are not limited by other considerations such as size, weight, etc.

A widely used form of the radar range equation is:

$$R_{\max}^4 = \frac{P_t G A_e s e^{2aR_{\max}}}{(4\pi)^2 S_{\min} L_s}$$

where

$P_t$  = peak transmitted power

$G$  = antenna gain

$A_e$  = effective antenna aperture

$s$  = radar cross section of the target

$S_{\min}$  = minimum detectable signal, watts

$a$  = atmospheric attenuation constant

$L_s$  = system losses

With the exception of  $s$  and  $a$ , all of these parameters are, at least theoretically, under the control of the system designer. However, in practice many of them are determined by secondary considerations. For instance,  $A_e$  and  $G$  are fixed by considerations such as antenna size, antenna beamwidth, sidelobe suppression, etc. and for purposes of this thesis, will be considered to be fixed. Likewise,  $L_s$  is not a truly adjustable parameter since it should be minimized in any system under consideration.

$S_{min}$  represents the weakest signal the radar receiver can detect and it is limited by the noise energy that occupies the same portion of the frequency spectrum as the signal energy. Some of this noise energy enters the receiver along with the desired signal. This environmental noise may be classified into cosmic noise, atmospheric absorption noise, atmosphere and man-made noise, and solar noise. Of these, cosmic noise is of by far the greatest significance at microwave frequencies.

Even if there were no noise accompanying the signal into the receiver, there would still be the noise energy in the receiver output which was generated in the receiver. This noise is mainly due to thermal noise, also known as Johnson noise, and shot noise. It can be practically eliminated by the use of low-noise receiver front ends such as microwave masers and parametric amplifiers. In this case the noise at

the receiver output is limited to the environmental noise and the thermal noise seen by the antenna.

Besides using low-noise receiver first stages, another method of reducing  $S_{\min}$  is to sum all the radar echo pulses returning from a target on one particular scan. This process is called interpulse integration, and its usefulness is due to the fact that the noise voltage averaged over the integration time-period, one scan in this case, has zero value while the signal voltages are additive. The most common radar interpulse-integration system is the cathode-ray-tube display combined with the integrating properties of the operator's eyes and brain, but either digital or analog electronic integrators could be built.

A second method of reducing  $S_{\min}$  using an integration scheme is to sum the energies contained in various portions of each transmitted pulse. This is known as intrapulse integration and is the basis for pulse-compression schemes, which can be analog, such as the FM chirp system, or digital, such as the phase-coded pulse-compression techniques, including those using complementary series.

Both interpulse and intrapulse integration can be considered as an increase in transmitted energy, since interpulse integration relies on the addition of energies contained in several short pulses and intrapulse integration relies on the addition of energy contained in several short subpulses of a single long pulse.

The last parameter in the radar equation to be considered is peak transmitted power. Increasing  $P_t$  would have the desirable effect of increasing the amount of energy transmitted in each pulse.

Tubes used for RF power generation take the form of either self-excited power oscillators, such as the magnetron, or power amplifiers, such as klystrons and traveling-wave tubes, driven by stable low-power oscillators. All tubes, whether power oscillators or amplifiers, suffer the same peak-power limitations imposed by voltage breakdown in waveguides or cavities. Peak transmitted power has been increased to the maximum possible value.

Besides peak power, the pulse duration has an effect on transmitted energy, since  $E_t = P_t \gamma$ . However, the limit to which pulse duration can be increased is set by the resolution requirements of the system. Increasing the pulse duration reduces the high-frequency content of the pulse, which has the effect of degrading range resolution. The solution to this dilemma has been to retain the high-frequency content of a narrow pulse by using intra-pulse modulation, which originally took the form of the FM chirp radar system.

Thus intrapulse integration, as noted above, is seen to be the motivation for intrapulse modulation, as intrapulse modulation has the effect of breaking the long pulse into short subpulses with the requisite high-frequency content. These subpulses can then be summed for detection, as required

in intrapulse integration. This basic idea, attributable to P. M. Woodward,<sup>1</sup> indicates that the transmitted pulse can be designed to be as wide as necessary to meet the energy requirements of the system, and that after the detectability requirement has been satisfied the range resolution conditions can be met by coding the transmitted signal with wideband modulation information. One of the most important contributions by Woodward to the development of modern radar technology was to point out that range resolution and accuracy were functions of the signal bandwidth, and not of the transmitted signal per se.

The extraction of the wideband information contained in an intrapulse-modulated pulse requires the use of a more complex receiving system than that needed for a simple short-pulse radar. These complex receiver systems are designated as matched-filter signal-processing systems.<sup>2</sup>

After a brief description of the FM chirp system, and an introduction to phase-coded pulse compression using binary series to modulate the transmitted waveform, this thesis will describe attempts to implement an intrapulse modulation-integration scheme using complementary series of length 4. Several such systems were built with varying degrees of success.

The next chapter looks at various pulse-compression, matched-filter, or coded-waveform techniques with the idea of eventual comparison of their characteristics to those of



the system built. Chapter 3 provides a familiarization with complementary codes and their ambiguity functions.

Chapter 4 describes the system as it was built in breadboard fashion in the laboratory, concentrating on concepts and leaving detailed description of circuits employed to be described in the appendices. Chapter 5 contains the summary, conclusions and suggestions for further study of pulse-compression systems using complementary series.

## II. PULSE COMPRESSION SYSTEMS

The original motivation to use pulse compression grew out of efforts during World War II to upgrade radar system performance. As the war progressed and radar receivers improved, it became obvious that the major impediment to further progress in improving radar performance lay in the power limitations of the transmitters being used.<sup>2</sup> On the other hand, range resolution could not be sacrificed by the use of wider pulse widths.

A method to avoid this dilemma was proposed by individuals on both sides of the conflict, and pulse compression, or waveform design, was born. However the concept arrived too late on the scene to be useful, as the war ended and there was little interest in pursuing development further until the early 1950's, when the chirp system was developed.

The basic idea was to transmit a wide pulse of constant amplitude and of duration  $\mathcal{T}$ , as shown in Figure 2.1a, during which the carrier frequency was linearly swept upward with time from  $f_1$  to  $f_2$  as shown in Figure 2.1b. This gives a large frequency bandwidth to the pulse while at the same time permitting the use of a long pulse duration. The time waveform of the output of the transmitter is shown in Figure 2.1c. Upon reception the signal is processed through a matched filter whose time-delay characteristic is the reverse of the frequency sweep; that is, the low frequencies are delayed more than the highs, as

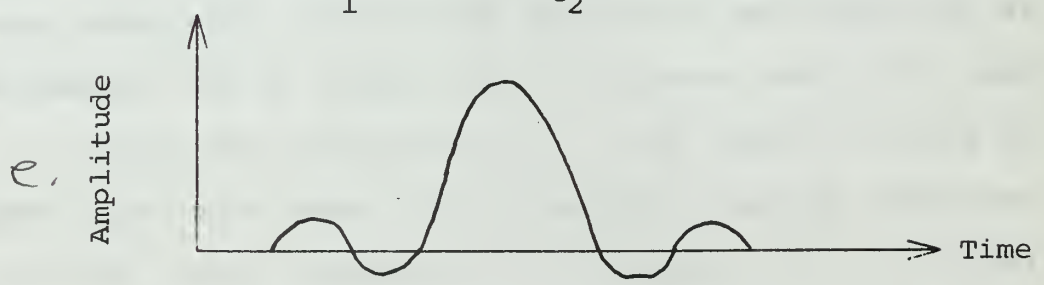
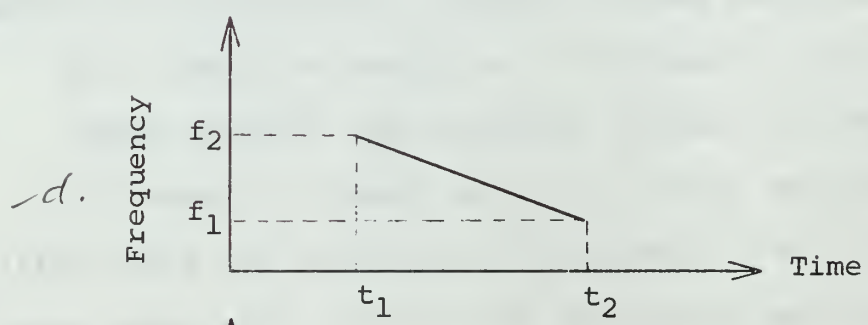
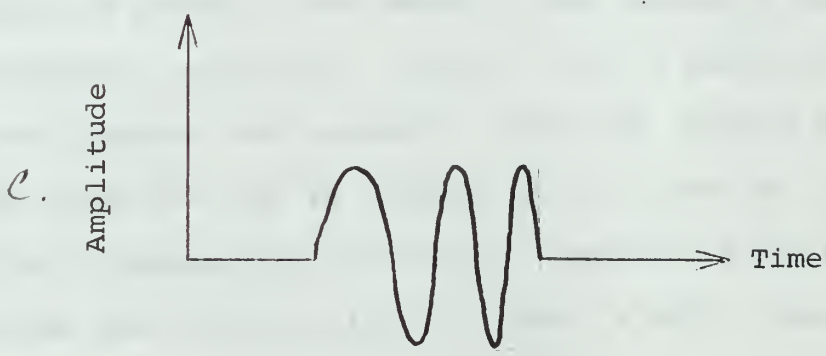
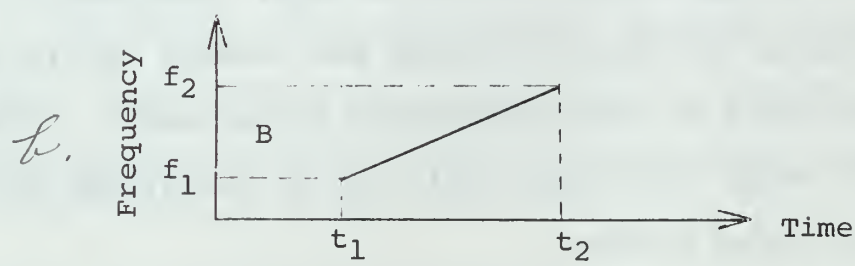
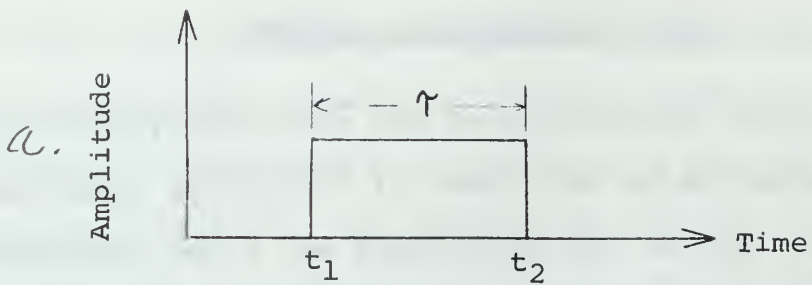


Figure 2.1. Frequency modulation of the chirp radar.

is shown in Figure 2.1d. The result is that all the energy contained in a long pulse of duration  $\gamma$  arrives at the filter output at the same time, producing a large, narrow output pulse of duration  $1/B$ , where  $B = f_2 - f_1$ , as shown in Figure 2.1e. The shape of the compressed pulse is proportional to  $(\sin \pi Bt)/(\pi Bt)$ .<sup>3</sup>

The time, or range sidelobes shown in Figure 2.1e are usually small enough with respect to the main lobe to avoid questions of ambiguity in measurement of range if there is only one target present. However, if there are many targets, having different radar cross sections, the sidelobes create a resolution problem since the sidelobes of a large target might hide the main lobe from a small nearby target. These range sidelobes can be reduced somewhat by using weighting filters.

The pulse-compression method described above is generally thought of as being an analog method. The digital method to be described next, attributed to B. Elspas,<sup>4</sup> uses phase-coded subpulses within the main pulse. A long pulse of duration  $\gamma$  is divided into  $B\gamma$  subpulses, where  $B$  is the bandwidth of the compressed pulse and depends on the range accuracy and resolution desired. Each of the subpulses is then of duration  $1/B$ , or  $\gamma/N$ , where  $N$  is the number of subpulses within the main pulse, and is equal to the time-bandwidth product of the waveform.

The phase of each of the subpulses is phase-modulated according to whether the corresponding position in a binary sequence has the value +1 or -1. An unchanged phase could represent a +1, for instance, and a complete inversion, or phase change of  $180^\circ$  could represent a -1.

Consider, for example, the transmitted pulse shown in Figure 2.2a. This pulse waveform was generated by using the binary sequence +1, +1, +1, -1, +1 to phase-modulate the carrier. How this might be done will be shown later. Upon being reflected from a target this waveform would be fed into a matched filter consisting of a tapped delay line and scaling adder as shown in Figure 2.2b. Figure 2.2c shows the signals in their correct time relationship as they arrive at the scaling-adder input. The output of the scaling adder is also shown. After phase detection, shown in Figure 2.2d, the signal is processed in the video section of the radar in much the same fashion as it is with short-pulse radar. It can easily be shown that the output of the phase detector is exactly the same as the autocorrelation function of the waveform.

There are three important features to be noted in the output of the matched filter. First, it is delayed in time with respect to the input, the delay being dependent on the code length. Secondly it has a central peak whose height is proportional to the code length. Lastly, there are range or time sidelobes present in the matched-filter output,

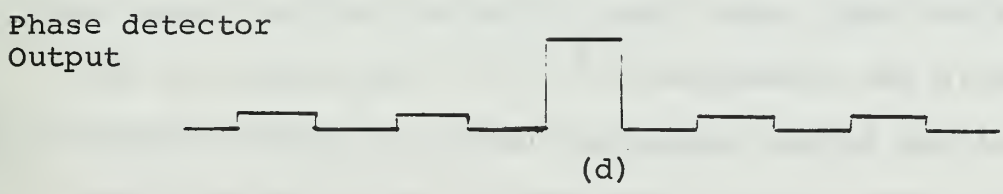
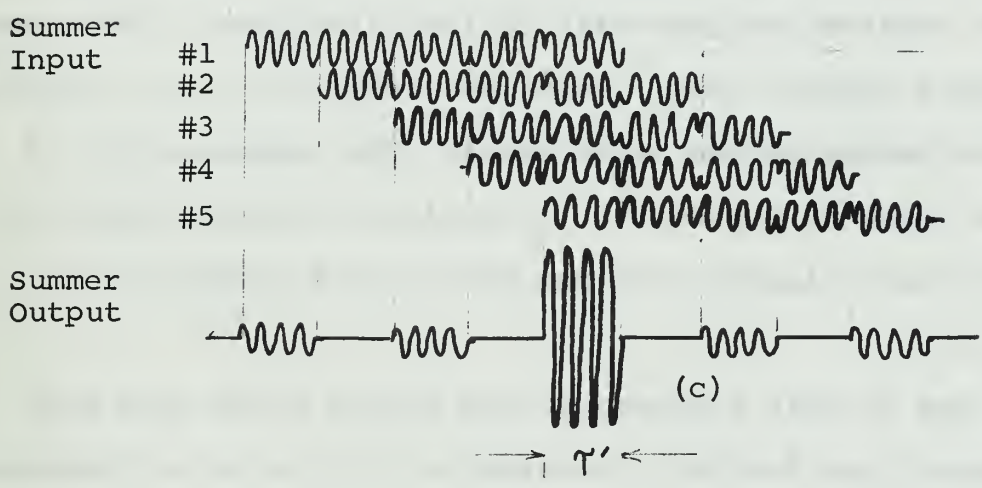
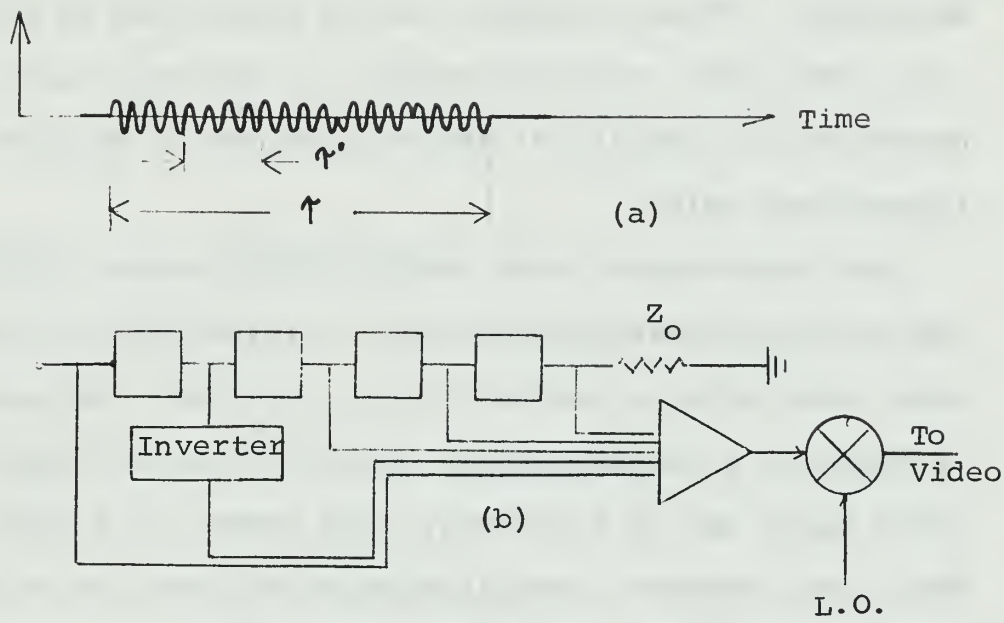


Figure 2.2. Autocorrelation of the binary Barker series of length five.

similar to those present in the linear FM system already described. These sidelobes can be classified as coding noise and their size with respect to the main lobe will depend on the quality of the code chosen to modulate the transmitted pulse

Any code chosen, even one picked at random, will exhibit the pulse-compression phenomenon illustrated in Figure 2.2 when received by a matched-filter receiver. One might ask if there is a certain binary code or class of codes for which there are no sidelobes. The answer is a qualified no. There are, however, certain classes of codes which are optimal for use as phase-modulating recipes, since these produce receiver outputs with minimum sidelobes. These are the binary Barker codes,<sup>5</sup> sometimes referred to as "perfect" words or pseudo-random noise codes. The complete list of them is shown in Figure 2.3. It will be observed that the Barker code of length five was used in the example in Figure 2.2.

So far in this discussion only binary codes have been considered, and further discussion will also be so restricted, with the exception of the present digression to mention two of the many other types of codes that have been described in the literature.<sup>5,6,7,8,9</sup> The first uses the Generalized Barker sequences, which are finite sequences of complex numbers having the absolute value of unity and multiple phases, depending on whether the codes are ternary,

<u>Length</u>	<u>Barker Code</u>
2	1,1
3	1,1,-1
4	1,1,1,-1; 1,1,-1,1
5	1,1,1,-1,1
7	1,1,1,-1,-1,1,-1
11	1,1,1,-1,-1,-1,1,-1,-1,1,-1
13	1,1,1,1,1,-1,-1,1,1,-1,1,-1,1

Figure 2.3. List of all known binary Barker codes.



quaternary, sextic, etc. The binary Barker codes are a special case of the generalized Barker sequences in which only  $0^\circ$  and  $180^\circ$  phases are allowed.

Another class of non-binary codes uses the Impulse-Equivalent pulse trains first proposed by Huffman.<sup>6</sup> In these codes the components of a pulse sequence are allowed to come from a continuum of values, rather than from a finite set. All are real-valued. The autocorrelation functions of these codes can be made to approach that of a single pulse as closely as desired. The process of generating them is extremely involved, however.

There does not seem to be a simply generated, that is, binary, code which, when received by a matched-filter receiver, will completely eliminate the range sidelobes or hash. A logical next step would be an attempt to find a pair of codes which, when simultaneously received by matched-filter receivers, have the property that the sidelobes of one are canceled by the sidelobes of the other. Code pairs of this type do indeed exist and are known as complementary codes.<sup>10</sup> These codes are formally defined and completely described in Chapter III. The methods of utilization of complementary codes to phase-modulate the transmitted pulse and matched-filter reception of these signals are exactly as already described for the binary Barker codes. The property of sidelobe cancellation is the prime advantage of complementary sequence pairs over other forms of binary code modulation.

Each of the pulse-compression methods described in this chapter has had the characteristic that the transmitted signal is wideband for good resolution and at the same time it is of long duration, for high pulse-energy content. It was exactly this characteristic that spurred development of pulse-compression, or coded-waveform techniques. Some of the practical benefits of pulse-compression systems are as follows:

1. More efficient use of transmitter power and avoidance of peak-power problems.
2. Increased system resolving capability, both in range and velocity, over that obtained by short pulse radar.
3. Enemy detection of wideband radar pulses is more difficult.
4. Jamming of a wideband, noise-like signal is much more difficult than jamming of a conventional radar signal.

Balanced against these benefits are the additional system complexity and cost. A decision will have to be made in any system design as to whether or not the final requirements of the system necessitate the use of pulse compression.

### III. COMPLEMENTARY CODES

Complementary codes, also known as complementary binary sequences, or complementary series, consist of "a pair of equally long, finite sequences of two kinds of elements which have the property that the number of pairs of like elements with any one given separation in one series is equal to the number of pairs of unlike elements with the same given separation in the other series."<sup>10</sup> This thought-provoking definition is best illustrated by an example, as follows. Consider the following complementary code pair:

A = -1, -1, -1, +1, -1, -1, +1, -1

B = -1, -1, -1, +1, +1, +1, -1, +1

Code A has three pairs of like adjacent elements, while B has three pairs of unlike adjacent elements. An element may be used in more than one pair. A also has four pairs of unlike adjacent elements while B has four pairs of like adjacent elements. Taking the illustration one step further, A and B also have, respectively, three pairs of like elements and three pairs of unlike elements if the pair members are required to be separated from their mates by exactly one element, and so forth for all the  $(N - 2)$  possible separations, where  $N$  is the number of elements in a series.

These codes have a great deal of mathematical structure and have been discussed at great length by Golay and

others.<sup>10,11,12</sup> They are binary and non-periodic. Golay showed that  $N$  must always be an even number and the sum of two squares. Considering these two restrictions, possible values for  $N$  up to 50 are 2, 4, 8, 10, 18, 20, 26, 32, 36, 40 and 50. The value  $N = 18$  has been eliminated by other considerations. Kernels, or basic code lengths which cannot be decomposed into shorter length codes, exist for codes of length 2, 10 and 26. S. Jauregui, in his doctoral thesis,<sup>12</sup> conducted an exhaustive computer search for the kernel of length 26 and a partial, inconclusive search for the next possible kernel, that of length 34. The search for the kernel of length 26 was successful, but Jauregui concluded that an exhaustive search for a kernel of length 34 was not feasible because it would require three million hours of computer time, based on using a CDC 1604 computer which accomplishes 200,000 operations per second.

The most useful property of complementary codes from the standpoint of this thesis is that, provided the two kinds of elements are +1 and -1, the sum of their individual autocorrelation functions is zero, except for zero shift, where it is equal to  $2N$ . That is, if the separate autocorrelation functions are given by

$$R_A(\gamma) = \sum_{i=1}^{i=N-\gamma} a_i a_{i+\gamma}$$

and

$$R_B(\gamma) = \sum_{i=1}^{i=N-\gamma} b_i b_{i+\gamma}$$

then

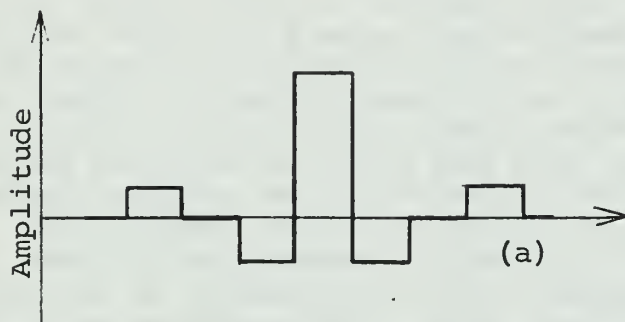
$$\begin{aligned} R_A(\gamma) + R_B(\gamma) &= 0 \text{ for } \gamma \neq 0 \\ &= 2N \text{ for } \gamma = 0 \end{aligned}$$

This property is illustrated in Figure 3.1, for the actual series which was used on the system described in Chapter IV. The implementation of hardware to generate a radar pulse containing subpulses whose phases were made to represent the elements of the series, as well as the matched filters for detecting the target echo, is described in Chapter IV. In Figure 3.1 the inputs to the matched-filter receiver are represented by dc voltages. In the actual application these pulses would, of course, by phase-coded RF pulses, as in Figure 2.2. The receiver output, shown in Figure 3.1c, demonstrates that the hash level is zero; that is, no range sidelobes exist. This absence of hash corresponds to zero coding noise or an infinite coding signal-to-noise ratio. It is precisely this feature that distinguishes complementary series pairs from all other forms of noise or pseudo-noise modulation methods.

A discussion of radar ambiguity functions in general, and those of complementary codes in particular, would be useful at this point. The radar ambiguity function, as formulated by Woodward, serves as a very useful radar

Code A = 1,1,-1,1

Autocorrelation function of Code A



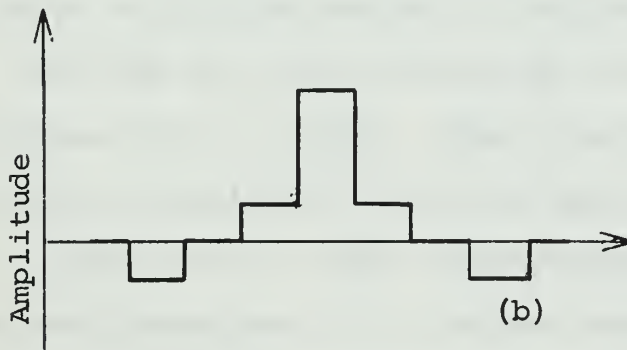
1	1	-1	1				
	-1	-1	1	-1			
		1	1	-1	1		
			1	1	-1	1	
1	0	-1	4	-1	0	1	

Time Shift

(a)

Code B = 1,1,1,-1

Autocorrelation Function of Code B



-1	-1	-1	1				
	1	1	1	-1			
		1	1	1	-1		
			1	1	1	-1	
-1	0	1	4	1	0	-1	

Time Shift

(b)



1	0	-1	4	-1	0	1	
-1	0	1	4	1	0	-1	
			8				

Time Shift

(c)

Figure 3.1. Autocorrelation of a complementary series.

waveform design criterion. It is a measure of range and doppler resolution. The ideal ambiguity function would be a delta function at the origin of the range, doppler axis.<sup>11</sup> Such a system would resolve two targets in range and doppler to an infinite degree, i.e. no ambiguities in either range or doppler. Of course this can never be achieved since it would require a pulse of infinite length composed of infinitely short subpulses, but nevertheless it is useful as a reference to which other ambiguity functions can be compared.

Loosely speaking, the ambiguity function of a waveform is identical to the output of the matched-filter receiver. However, this intuitive definition cannot be applied directly to complementary codes. Akita, in his master's degree thesis,<sup>11</sup> extended Sievert's definition of the ambiguity function to complementary codes for two cases, wideband and narrowband analysis. By narrowband analysis it is meant that the doppler effect does not significantly alter the envelope of the transmitted signal. Akita defined the ambiguity function of a complementary code, in the narrowband case, to be the sum of the ambiguity functions of the individual members of the complementary pair. Therefore the range sidelobes for the complementary-coded ambiguity function will be nonexistent for zero doppler frequency. There are, however, range ambiguities at other doppler frequencies, and doppler ambiguities may exist at all ranges.

In the wideband analysis case the doppler effect does alter the envelope of the transmitted signal. This alteration is insignificant, though, until the product of the target velocity and the waveform time-bandwidth product approaches one-half the propagation velocity in the medium. Wideband analysis would therefore not apply unless extremely fast targets were being tracked by a radar using a very long pulse modulated by a long binary sequence.



#### IV. DESIGN, CONSTRUCTION AND EVALUATION OF A COMPLEMENTARY SERIES PULSE-COMPRESSION RADAR

##### A. GENERATION OF PHASE-CODED PULSES

One of the most easily instrumented methods of modulating an RF pulse according to a binary sequence, using the phase-reversal method of modulation is that of feeding a gated RF pulse into a tapped delay line, as shown in Figure 4.1. In this figure the sequence to be represented is again the binary Barker sequence of length five.

The delay line shown in Figure 4.1 is a distributed-parameter delay line and might be constructed of coaxial line, heliax, or stripline. It could also be an ultrasonic delay line, although tapping such a line might present problems. The delay lines used to generate phase-modulated pulses in this project were of the discrete or lumped parameter type, that is, LC sections. The complete design details of these lines are presented in Appendix A.

The output of the summer in Figure 4.1 is a phase-coded pulse of total pulse duration  $\gamma$ , and is composed of  $N$  subpulses, each of duration  $\gamma'$ , where  $\gamma' = \gamma/N = 1/B$ , where  $N$  is the number of digits in the binary sequence, and  $B$  is the bandwidth of the subpulse. A distinctive feature of Figure 4.1 is that the subpulse width is exactly equal to the length in microseconds of the delay line between taps. This insures a continuous RF pulse, with no gaps or overlaps. Figure 4.2 is a photograph of an actual pulse generated on

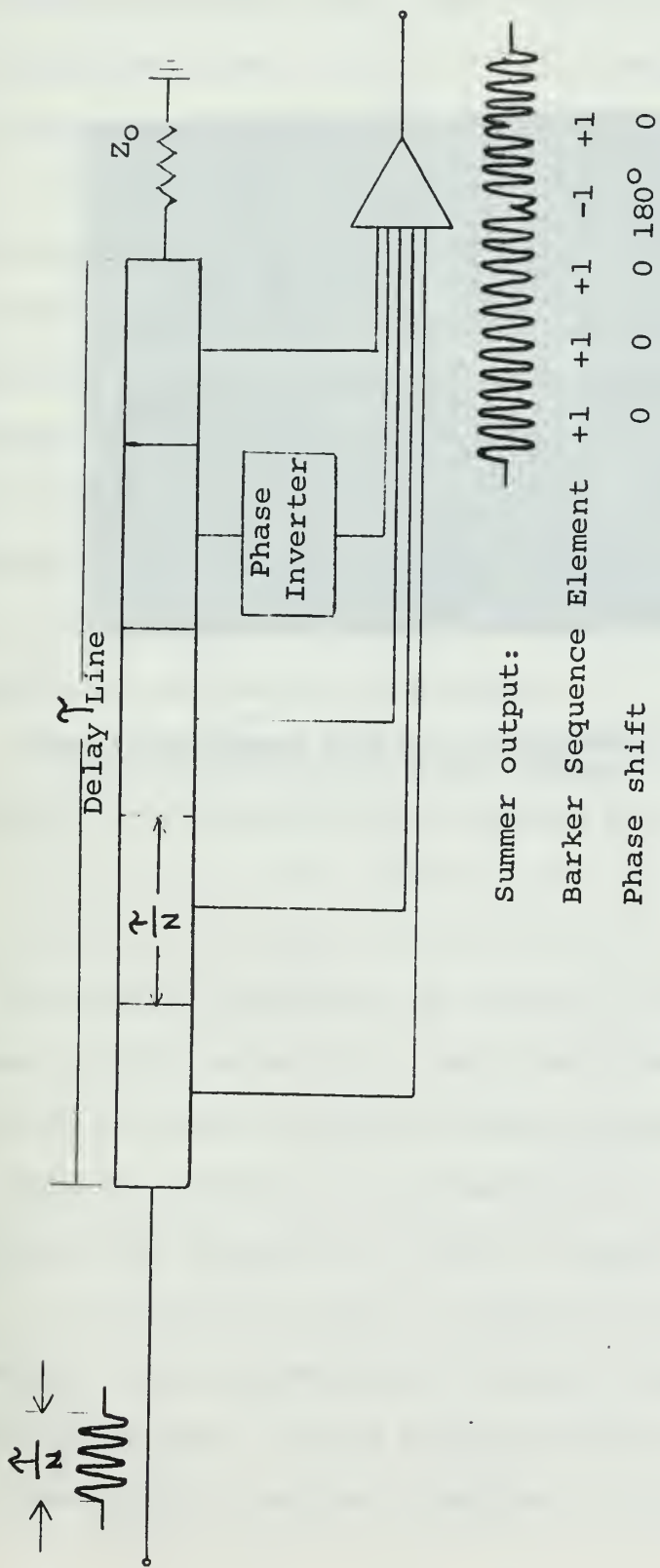


Figure 4.1. Generation of the five-digit Binary Barker Sequence.

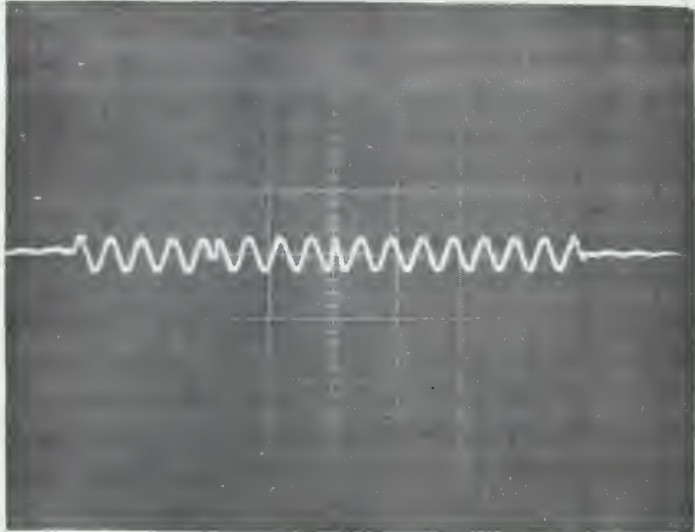


Figure 4.2. Photograph of pulse generated by the tapped delay line of Figure 4.3.

a tapped delay line in which  $\tau' = 2$  microseconds and the carrier frequency was 2 Mhz. The modulating binary sequence in this case was +1, +1, -1, +1. The phase reversal of the third subpulse stands out quite clearly.

Pulses similar to that in Figure 4.2 could be shifted to an appropriate microwave frequency, amplified by a klystron or TWT high-power amplifier and transmitted. As has been pointed out, the implementation of complementary-series pulse compression requires the transmission of both sequences of the complementary pair. Both of these sequences can be transmitted through one output tube with a moderate bandwidth, for example by using slightly different carrier frequencies for the two sequences.

The modulators built for this project were designed to generate the complementary series pair

$$A = +1, +1, -1, +1$$

$$B = +1, +1, +1, -1$$

A delay line length of  $(N - 1) * (\tau')$  is required to generate each of the sequences. The A and B pair above would each require 6 microseconds of delay, since it was decided to use a subpulse width of 2 microseconds. This choice gives range resolution comparable to that of many current search radars.

The subpulse width for precision radars such as for fire control would probably be made much smaller, possibly by a factor of ten. In the present application it was convenient to work with a carrier frequency of two Mhz, which permits

four complete cycles of carrier signal per subpulse. A higher carrier frequency would have made the design project much more difficult for several reasons. The main reason is that lumped-parameter delay lines have a lower cutoff frequency of  $f_{CO} = 1/\pi T_S$ , where  $T_S = (LC)^{1/2}$  and is the time delay per section of the line. For good results it is desirable for the ratio of the carrier frequency to the cutoff frequency to be less than one-half. Thus a carrier frequency of two Mhz requires approximately 50 LC sections of delay line per subpulse. Obviously a high carrier frequency was not feasible in this project because of the large number of inductors and capacitors required for the delay lines.

Since a total delay of 12 microseconds was needed just to generate the transmitted pulses and an additional 12 microseconds of delay to serve as the matched filter, a total of 660 LC sections requiring 660 inductors and 660 capacitors would have been required. Therefore an alternate means of generating the transmitted pulses was sought.

#### B. PROPOSAL USING A SINGLE DELAY LINE TO BOTH GENERATE AND RECEIVE THE PULSES

At this point the possibility was considered of using the same delay line to both generate the transmitted pulse and serve as the matched filter upon reception of the target echo. This has been proposed in the literature,<sup>13</sup> and the block diagram for one half of such a system is shown in Figure 4.3. The other half would be identical except that

the location of the inverters on the delay line would be different. It has been shown that in order to correctly autocorrelate a pulse which has been phase-reversal modulated, it is necessary for the autocorrelating delay line to have its taps arranged in reverse order as compared to the order of the taps on the generating delay line. This requirement is met by feeding the received signal in at the opposite end of the line. Switch #1 in Figure 4.3 would always be in the receive position (position 2) except during actual transmission of the transmitted pulse, when it would be at position 1.

This method would work quite satisfactorily for a complete radar in which the transmitted pulses were radiated from an antenna and received after having been reflected from a real target, as in Figure 4.3. However, in this project, the "transmitted" pulses were never actually transmitted but instead were fed directly back into the receiver as shown in Figure 4.4. Therefore if the same delay line were used to both generate the transmitted pulse and autocorrelate the received pulse, it would be necessary to build a target range simulator consisting of another delay line which would have to be a minimum of eight microseconds long to prevent the "received pulse" from entering the far end of the delay line prior to the time that the transmitted pulse had passed completely through. If this range simulator was built in the form of a lumped-parameter delay line,

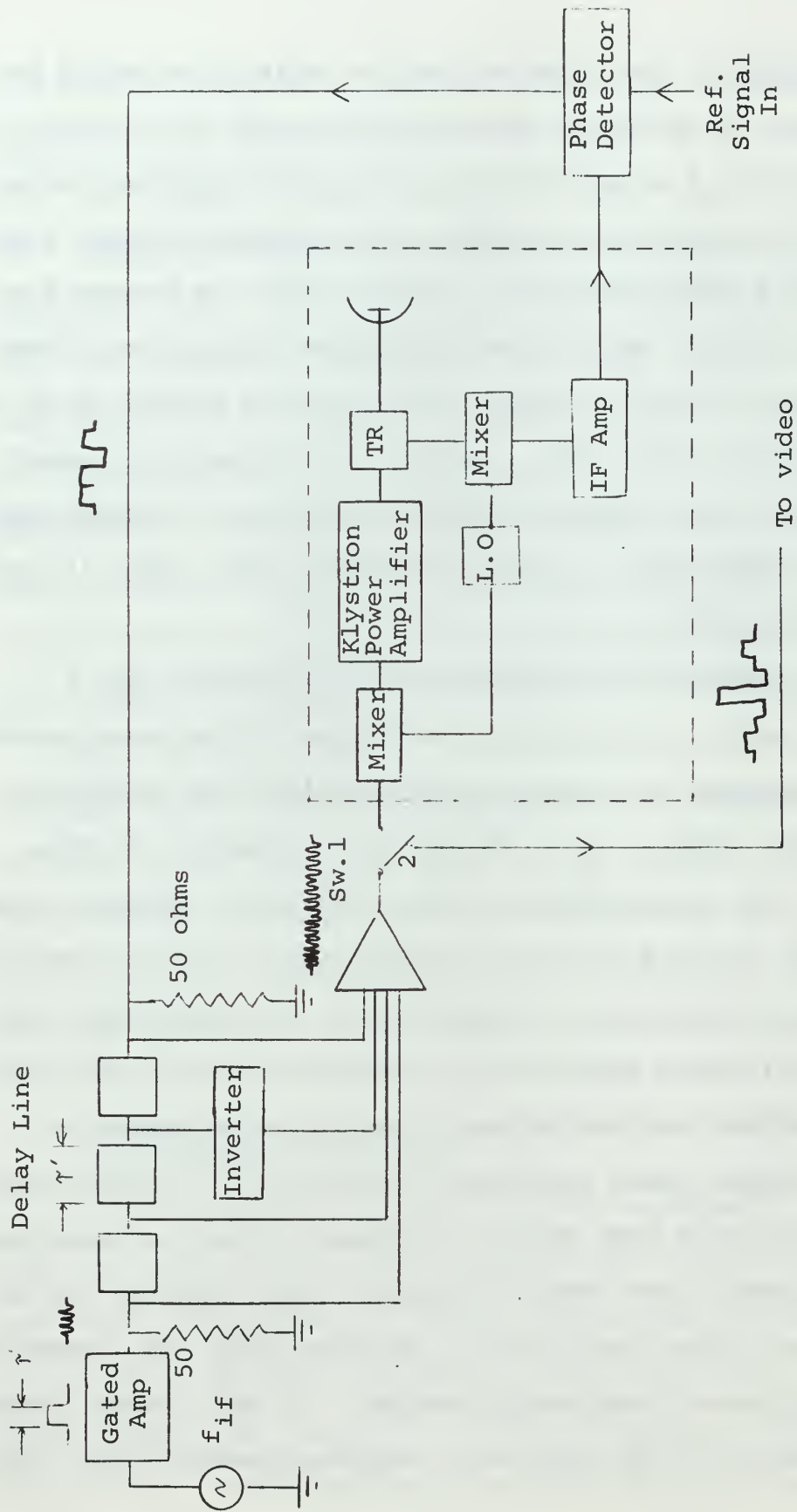


Figure 4.3 Single delay-line pulse generator-autocorrelator.

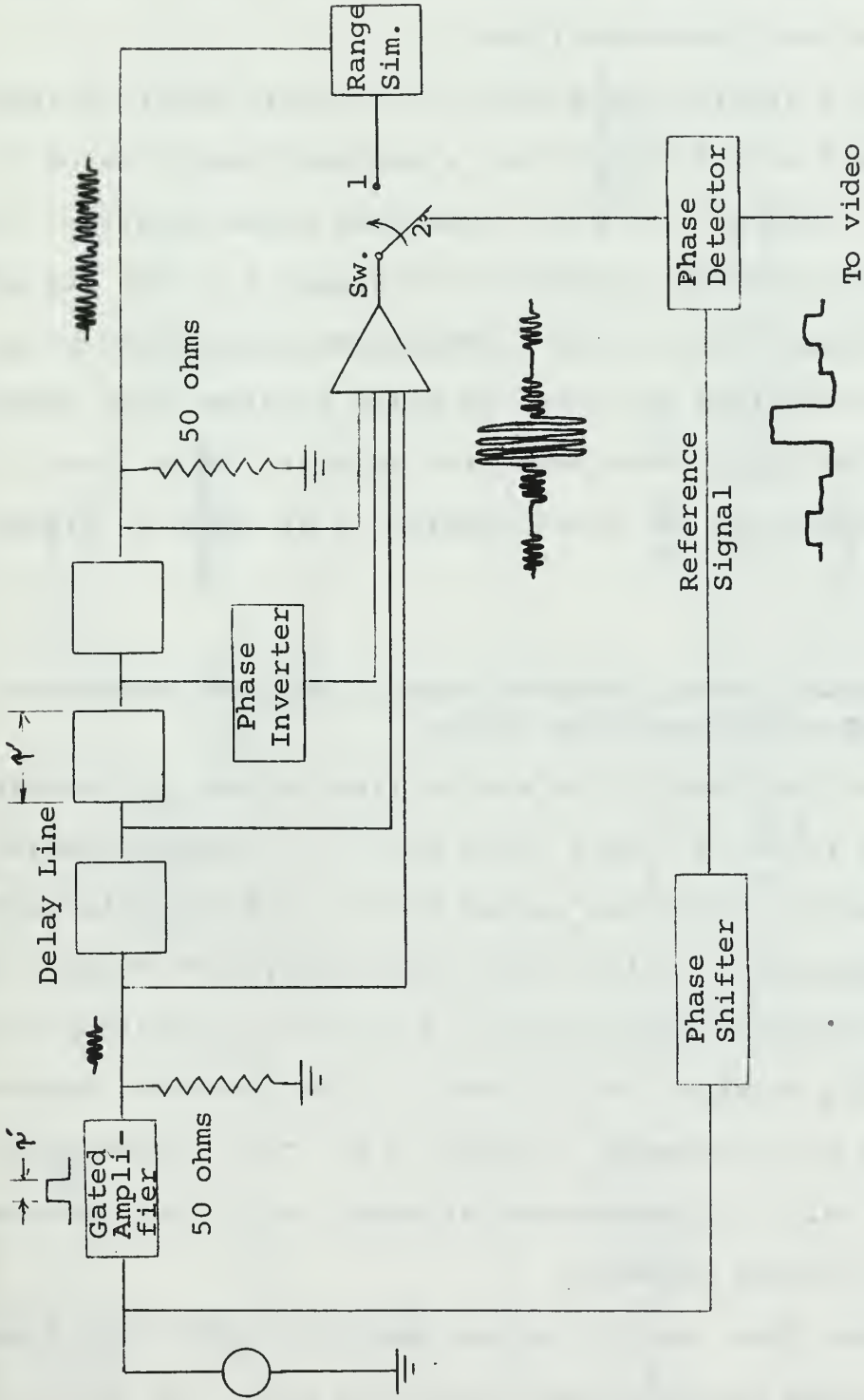


Figure 4.4. Laboratory model of the system in Figure 4.3



200 LC sections would be required. Perhaps a better simulator could be built by using coaxial line with a suitable amplifier and phase equalizer.

Such a single-line system, if actually built as shown in Figure 4.3 or 4.4, would have a minimum range time of  $\gamma$  seconds, where  $\gamma$  is the transmitted pulse duration. Under the semi-artificial conditions of Figure 4.4, the use of a single delay line to both generate the transmitted pulse and autocorrelate the received pulse requires more total delay-line length than using two separate delay lines, a system for which the block diagram is as shown in Figure 4.5.

#### C. PROPOSALS USING SEPARATE DELAY LINES FOR GENERATING AND AUTOCORRELATING PULSES.

As in the case of the single-line method, if the system shown in Figure 4.5 were to be built in a limited project, the elements inside the dashed block could be replaced by a range simulator. Unlike the single-delay-line method, the range simulator could consist of a direct connection, thus simulating a range time of zero. It is therefore omitted from the block diagram in Figure 4.6. This system would require only 12 microseconds of delay, or 300 LC sections for each binary sequence.

Rather than use the system shown in Figure 4.6, a system was designed in which the transmitted pulse was generated by a bank of four gated amplifiers all fed by the same

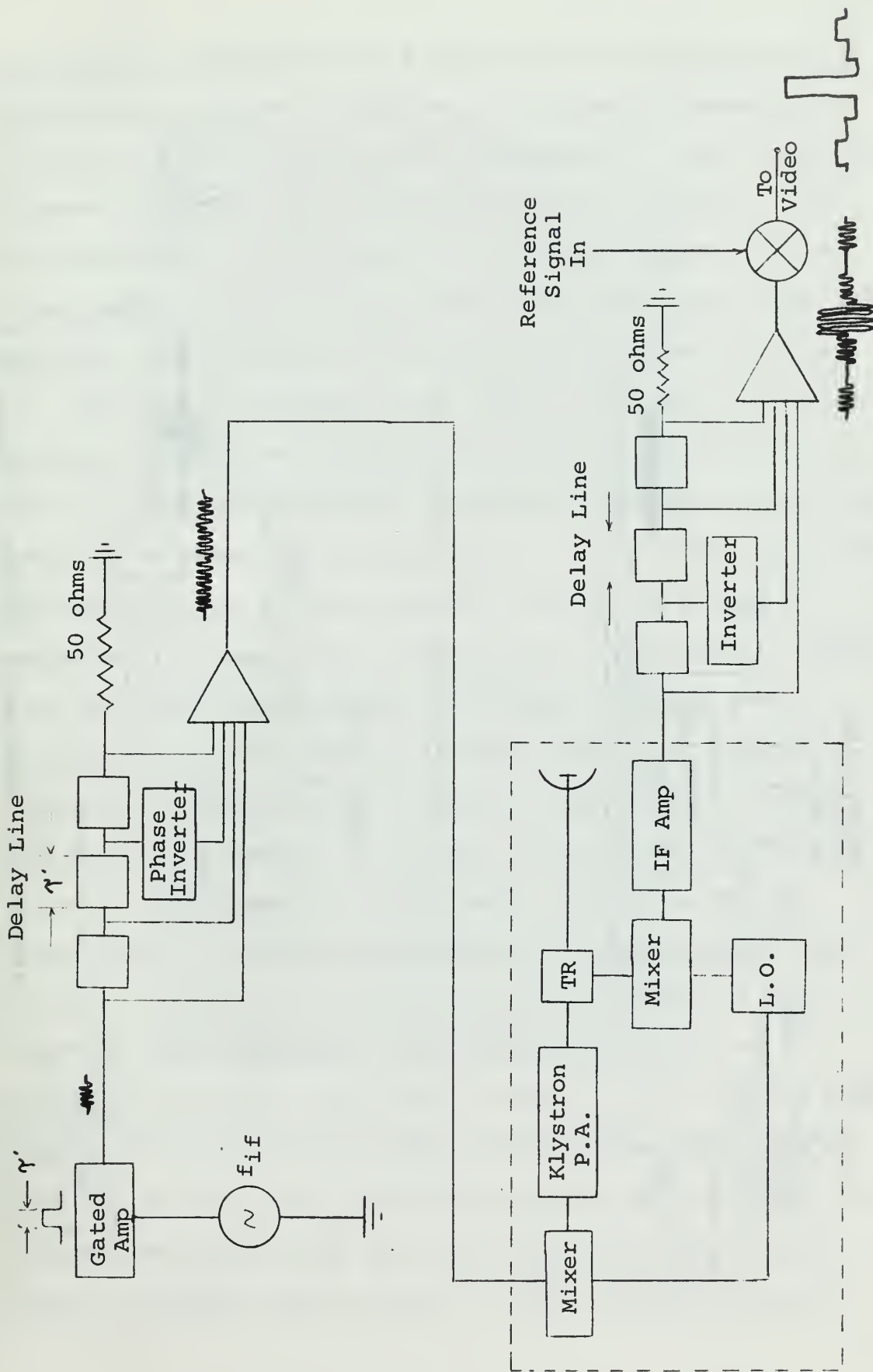


Figure 4.5. Pulse compression using separate delay lines to generate and autocorrelate waveforms.

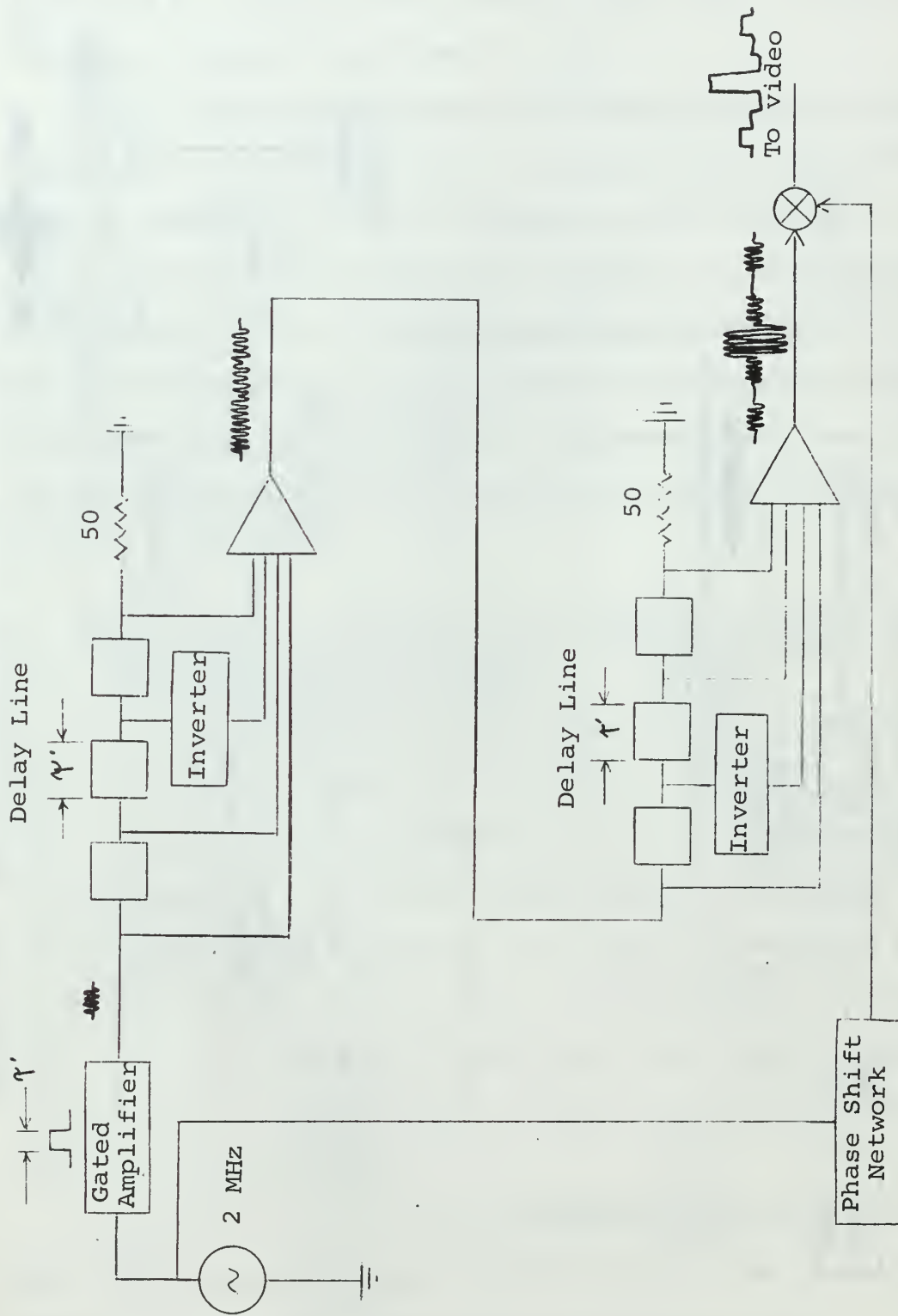


Figure 4.6. Laboratory version of Figure 4.5

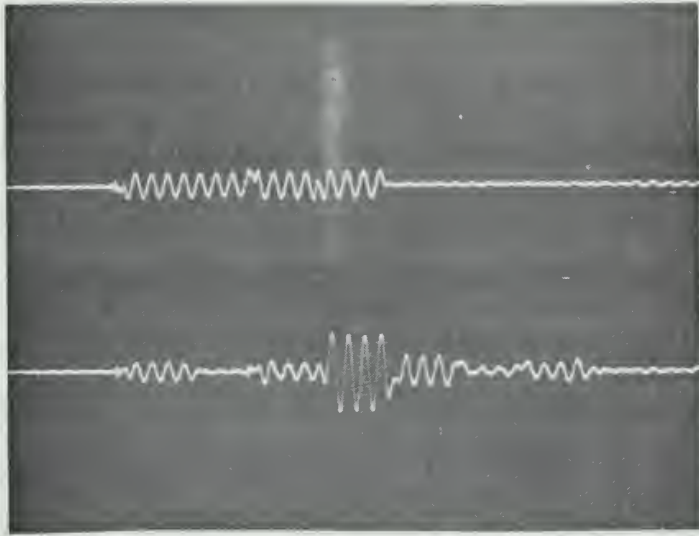
oscillator, but gated on and off by pulse generators which incorporated delayed triggering. The complete description of this circuitry is provided in Appendix D. This modulator reduced the delay-line requirements of the project to six microseconds or 150 LC sections for each sequence of the complementary pair. Actually the delay lines were made 165 sections long to provide some isolation from end effects.

The systems in Figures 4.4 and 4.6 were both built and tested. The system in Figure 4.4 was soon abandoned in favor of the one in Figure 4.6 for four reasons. First, it required an extra two microseconds of delay time. This was manageable while working with only one of the binary sequences, but would have required 28 microseconds of delay line for the entire project. Secondly, problems were encountered in the switch, although these were eventually surmounted. This switch is shown in Appendix B. Thirdly, the control of reflections on the line was very difficult, since it was being fed at each end. Lastly, as in any lossy line, the signal was attenuated as it travelled down the line. This meant that the fourth subpulse was smaller than the first subpulse. This attenuation could be corrected by adjusting the input resistors of the scaling adder used to sum the four subpulses. The problem with this is that if the input resistors are correctly adjusted for the transmitted pulse, they are wrong for the received pulse, since it travels down the line in the reverse direction.

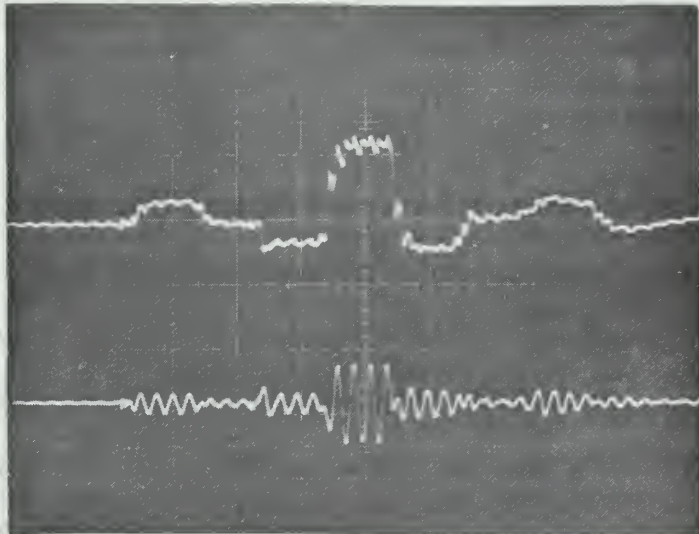
This problem could be alleviated by using one of the switches described in Appendix B for each tap on the delay line, and using separate scaling adders to sum the transmitted pulse and the received pulse. This was not attempted in view of the other deficiencies of the system.

The next approach was to build the system of Figure 4.6. This system produced the waveforms shown in the photographs in Figure 4.7. These waveforms compare quite favorably with their theoretical counterparts shown on the block diagram in Figure 4.6.

One of the chief problems encountered with this system was in getting the pulses coming off the four taps of the autocorrelator to add exactly in phase. Of course for this to occur it is required that there be exactly the same amount of delay between any two adjacent taps of a line as there is between any other two adjacent taps of the same line, and furthermore that the generating and autocorrelating delay lines be exactly alike. Since the buffering amplifiers and the phase inverters introduce some phase change, the phases of the waveforms coming off each tap had to compare exactly not at the point where the line was tapped but at the input to the scaling adder, at which point further relative phase changes could not occur. In order to obtain exact phase comparisons at the inputs to the scaling adders, it was necessary to insert LC sections of exactly the right delay time and 50 ohm impedance into the lines at



(a)



(b)

Figure 4.7. The top photograph shows the transmitted pulse in the top sweep and the output of the autocorrelator in the bottom sweep for the system in Figure 4.6. The bottom photograph shows the phase-detector output in the top sweep, with the autocorrelator output repeated for comparison in the bottom sweep.

the tapping points. It proved to be almost impossible to simultaneously match the 50-ohm impedance and correct the phase exactly. This is one of the reasons why the main lobe in the autocorrelation function shown in Figure 4.7 is not exactly four times the height of the sidelobes, as it should theoretically be. The second reason is that reflections on the lines due to seemingly unavoidable mismatches added in random fashion to the signal, causing it to be degraded.

The system in Figure 4.6 was therefore changed to that shown in Figure 4.8. The major difference is that phase detection of the received pulse is done prior to autocorrelation. The results, Figures 4.9 and 4.10, show a significant improvement. The reason is that the signals being summed by the autocorrelator's scaling adder were no longer required to add in phase, since they were only step functions. This meant that the requirement for the two delay lines to be exact duplicates no longer applied. The waveform in Figure 4.10 was obtained by using the B sequence, +1, +1, +1, -1 to phase modulate the transmitted pulse. This was physically accomplished simply by moving the inverter on the modulating line from the third tap to the fourth tap, and moving the inverter on the autocorrelator from the second tap to the first tap. Using this setup the transmitted and received pulses could be observed for both the A and B sequences, but not simultaneously. Therefore the cancellation of the range sidelobes could not be

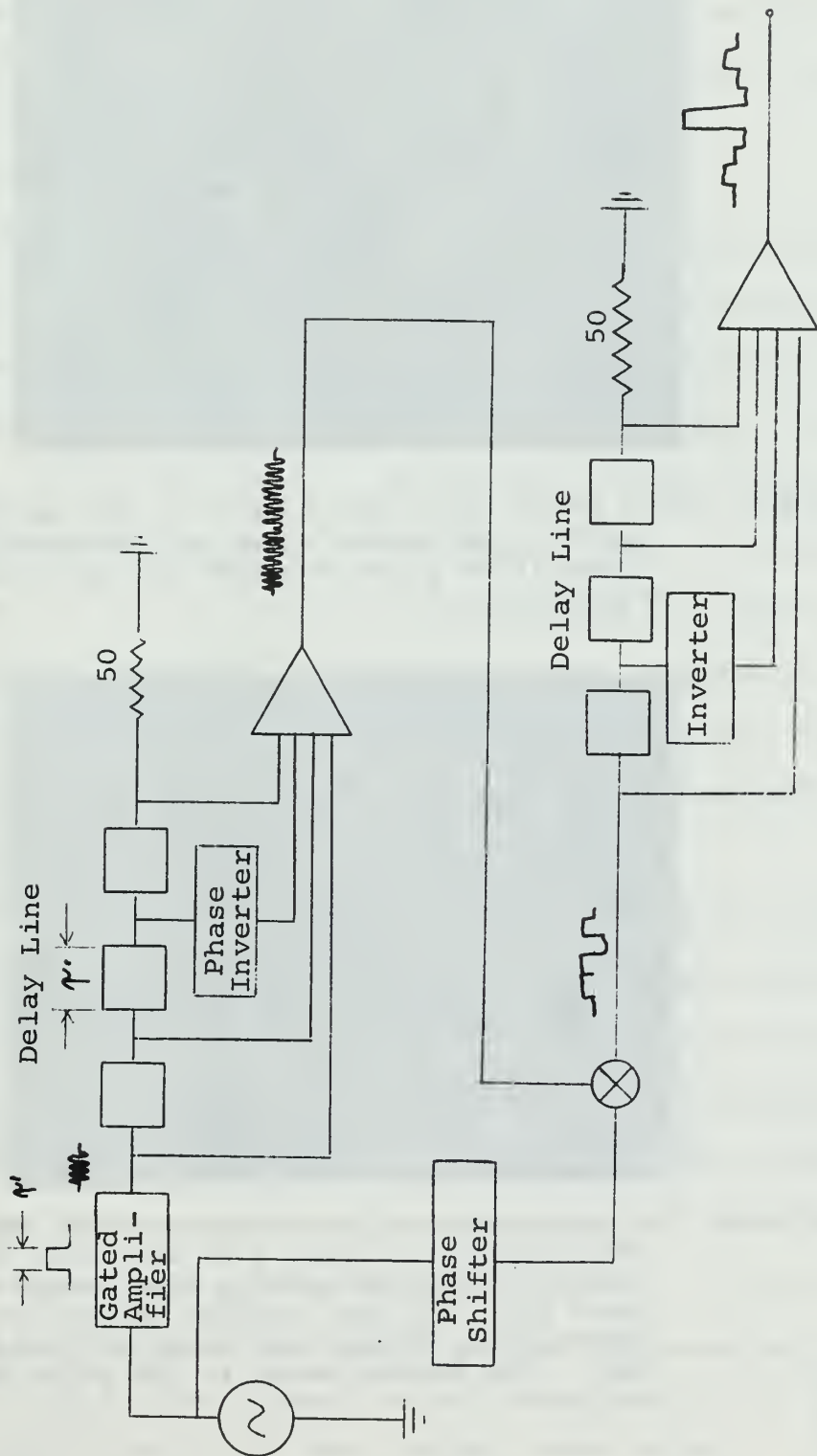


Figure 4.8. Phase detecting is done before autocorrelation in this system, as compared to Figure 4.6. Note the difference in waveforms entering the second delay line in the two figures.



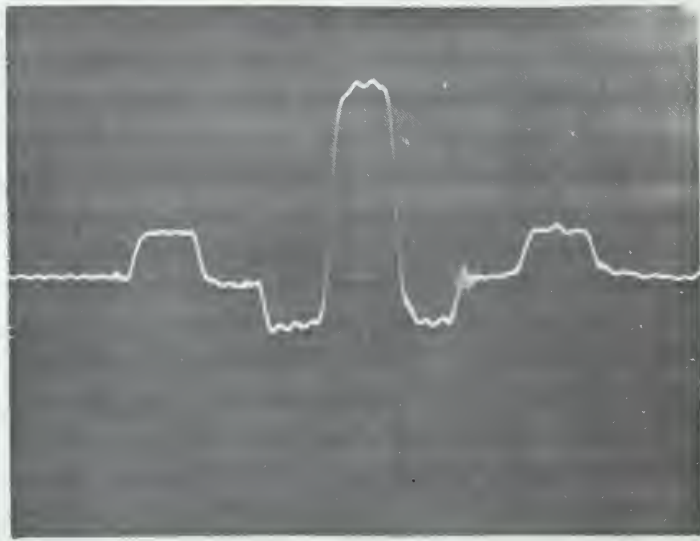


Figure 4.9. This photo shows the output of the autocorrelator for the system shown in Figure 4.8. The transmitted pulse was the same as that in Figure 4.7a.

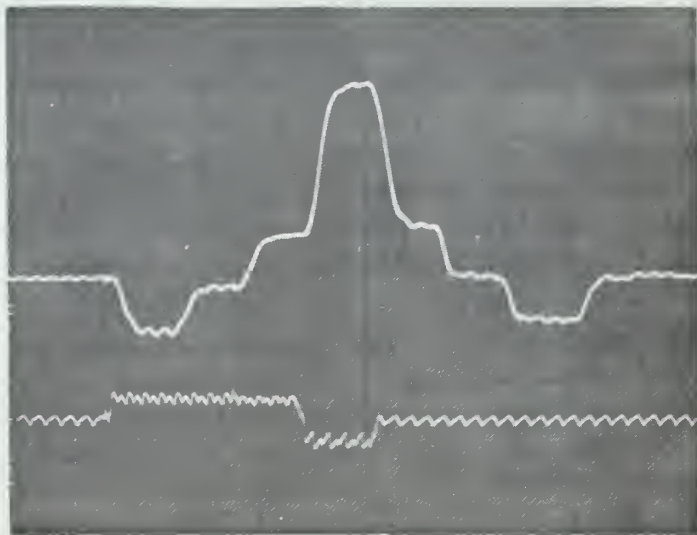


Figure 4.10. The top sweep is the autocorrelator output for the system of Figure 4.8, but with the inverter on the generating line moved to the last tap, and the inverter on the autocorrelating delay line moved to the first tap. The bottom sweep is the phase detector output.

observed directly. It was this consideration that motivated the search for a method to generate the transmitted pulses by some means other than delay lines. The modulator described in Appendix D was the result of this search.

#### D. FINAL CONFIGURATION

Use of the modulator described in Appendix D allowed the simultaneous generation and reception of both sequences without the necessity of having to build additional delay lines. It remained only to build an additional scaling adder to sum the outputs of the two autocorrelators. The final configuration of the system is shown in Figure 4.11 and 4.12. All of the circuits shown in the block diagrams are fully described in the Appendices. Outputs of the individual autocorrelators and the final output showing sidelobe cancellation are shown in the photographs of Figures 4.13 and 4.14.

The final output pulse is two microseconds wide, while the transmitted pulse was eight microseconds in duration. The ratio of amplitudes of the matched-filter output to the amplitude of the received signal is 8:1. In general it will be  $2N:1$ , where  $N = B\mathcal{T}$  and corresponds to the number of digits in the modulating binary sequences. The quantity  $B\mathcal{T}$  is defined as the pulse-compression ratio. It is clearly dependent only on the length of the complementary series used. While the largest kernel is of length 26, there is a distinct possibility that larger codes exist.

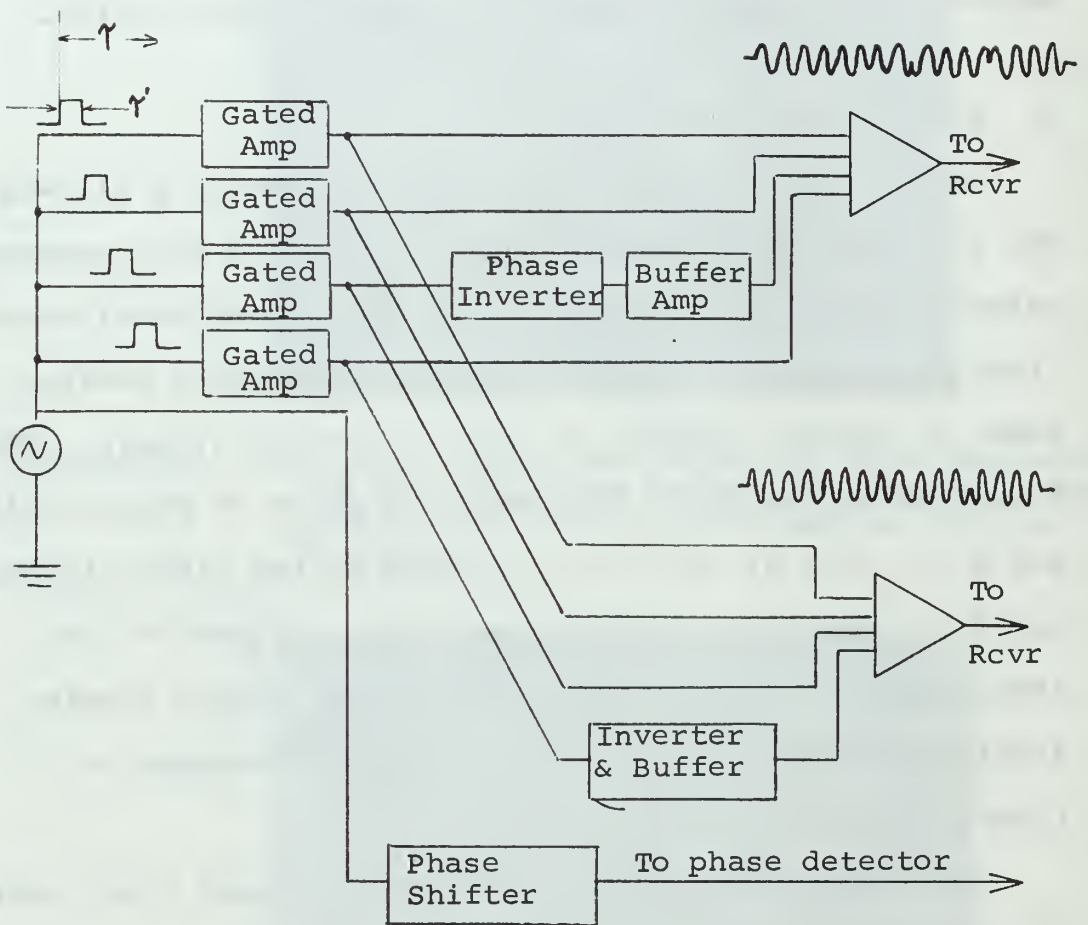


Figure 4.11. Final configuration of the pulse generator, showing generation of both sequences of the complementary pair  $A = 1, 1, -1, 1$  and  $B = 1, 1, 1, -1$ .

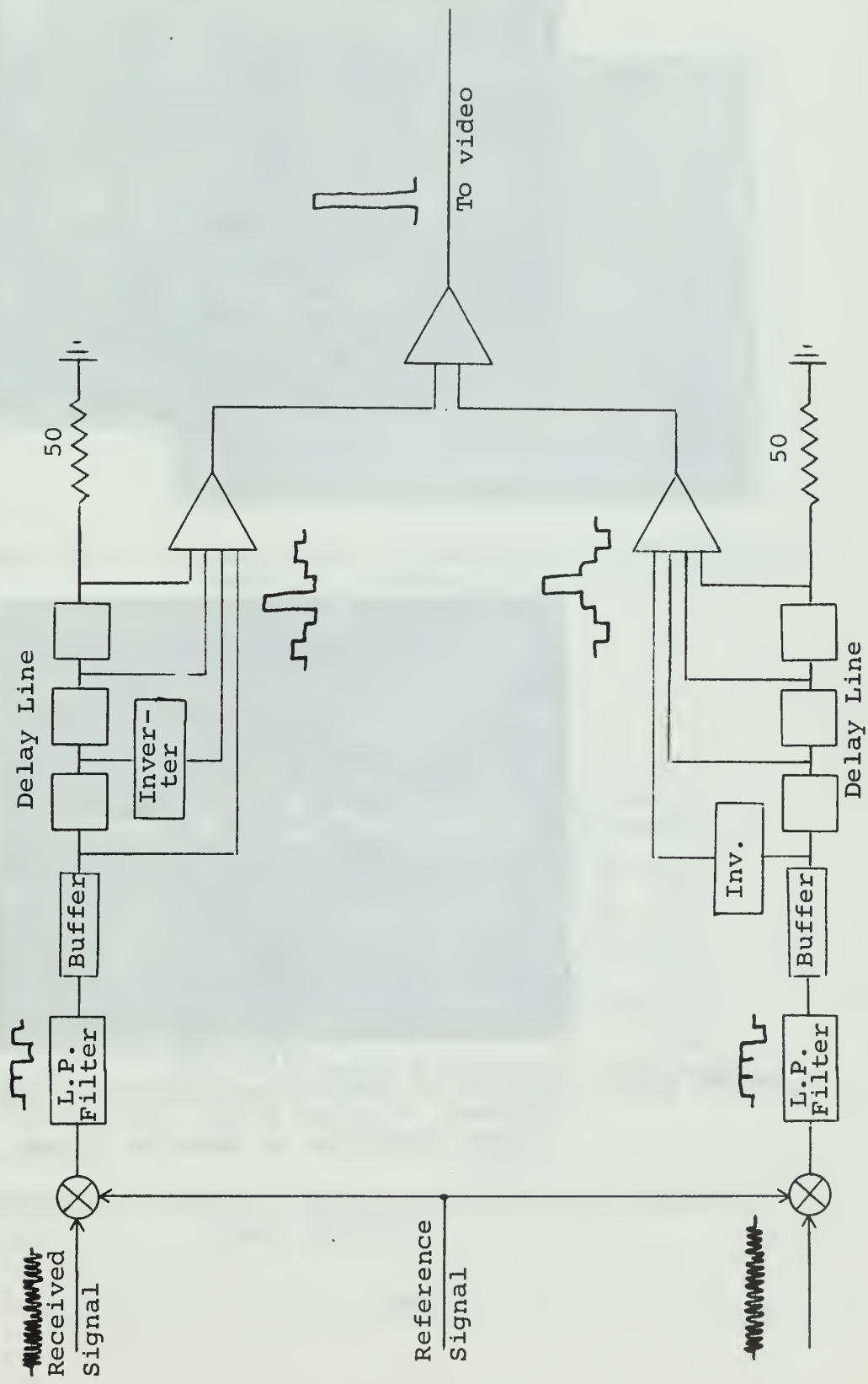
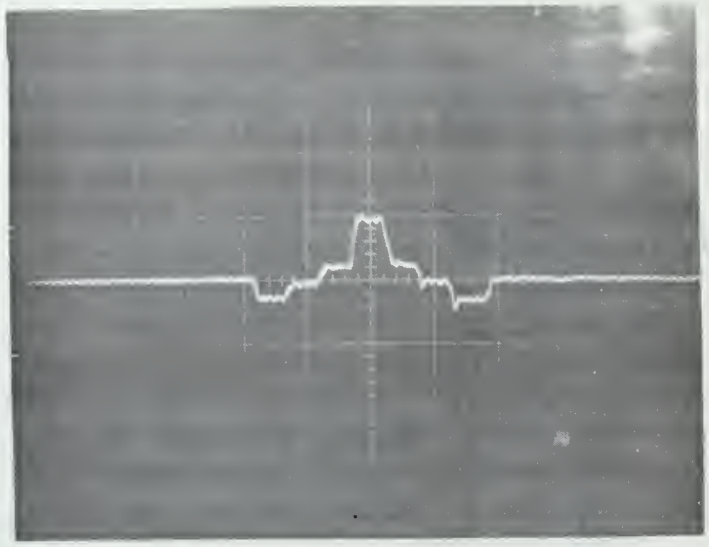
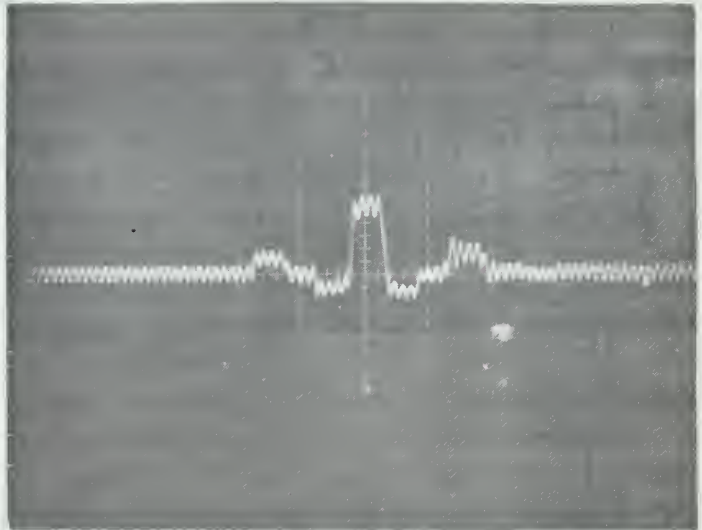


Figure 4.12. Final configuration, showing autocorrelation of both sequences of the complementary pair generated as in Figure 4.11.



(a)



(b)

Figure 4.13. Outputs of the autocorrelators of the system in Figure 4.12. The sum of these waveforms is shown in Figure 4.14.

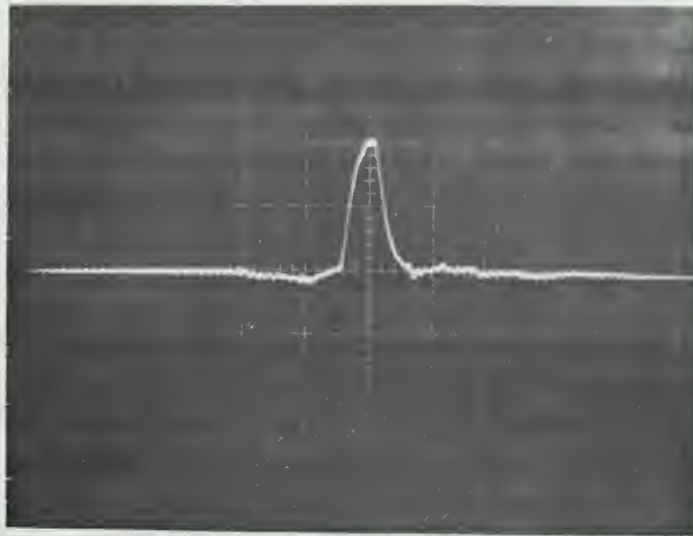


Figure 4.14. Final output of the system of Figures 4.11 and 4.12, showing the cancelation of range sidelobes.

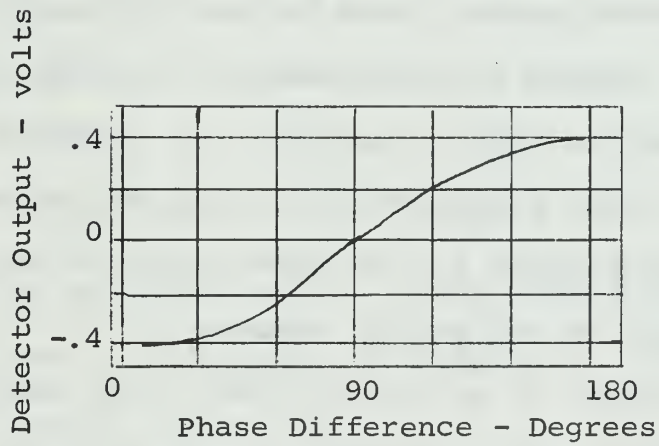


Figure 4.15. Output characteristics of the Relcom M1 phase detector.

As shown in Figure 4.12, it is necessary to phase detect the received pulse. This can actually be done either prior to autocorrelation or after autocorrelation, but the former method was found to be much more easily instrumented. The phase detector used was manufactured by Relcom and is described in Appendix G. Its output as a function of phase difference is indicated in Figure 4.15. One of the input signals is the received signal, the other is a reference signal, taken in this case to be the carrier frequency  $f_t$ . Reference to Figure 4.15 shows that for the output of the phase detector to be a positive maximum, corresponding to a +1 in the binary sequence, the input signals must be  $180^\circ$  out of phase. This was no problem in the artificial system built as shown in Figure 4.11 and 4.12 since the phase of the "received" pulse could be measured with respect to the reference signal and the phase of the reference signal could be adjusted so that it was  $180^\circ$  out of phase with the portion of the received pulse which was supposed to produce a positive maximum at the phase detector output, i.e., a +1 position in the binary sequence.

Of course, in an actual system like that shown in Figure 4.3 or 4.5, the phase of the received signal is unknown; in fact it is continuously changing if the target is moving radially with respect to the radar. It would be impossible to change the reference signal from one received pulse to the next so as to insure phase opposition between the

reference signal and the subpulses corresponding to +1 elements in the binary sequence. One way to overcome this problem would be to use quadrature detection, that is to detect the received pulse using two reference signals which are in time quadrature. The outputs of the two phase detectors would then be summed. However this was not instrumented due to lack of time, and for another reason to be explained later.

#### D. MTI COMPATIBILITY

The absence of knowledge of the phase relationship between the received signal and the reference signal is not a deficiency--in fact, it makes this system a natural for MTI or pulse-doppler use.

The block diagram for a simple MTI short-pulse radar is given in Figure 4.16. The coho, or coherent oscillator output voltage is the reference signal, and can be represented as

$$V_{\text{ref}} = A_1 \sin [2 \pi f_c t]$$

where  $A_1$  is the amplitude and  $f_c$  is the coho frequency, which is the same as the radar IF frequency. The doppler-shifted echo signal voltage is

$$V_{\text{echo}} = A_2 \sin [2 \pi (f_c + f_d) t - 4 \pi f_t R_0 / c]$$



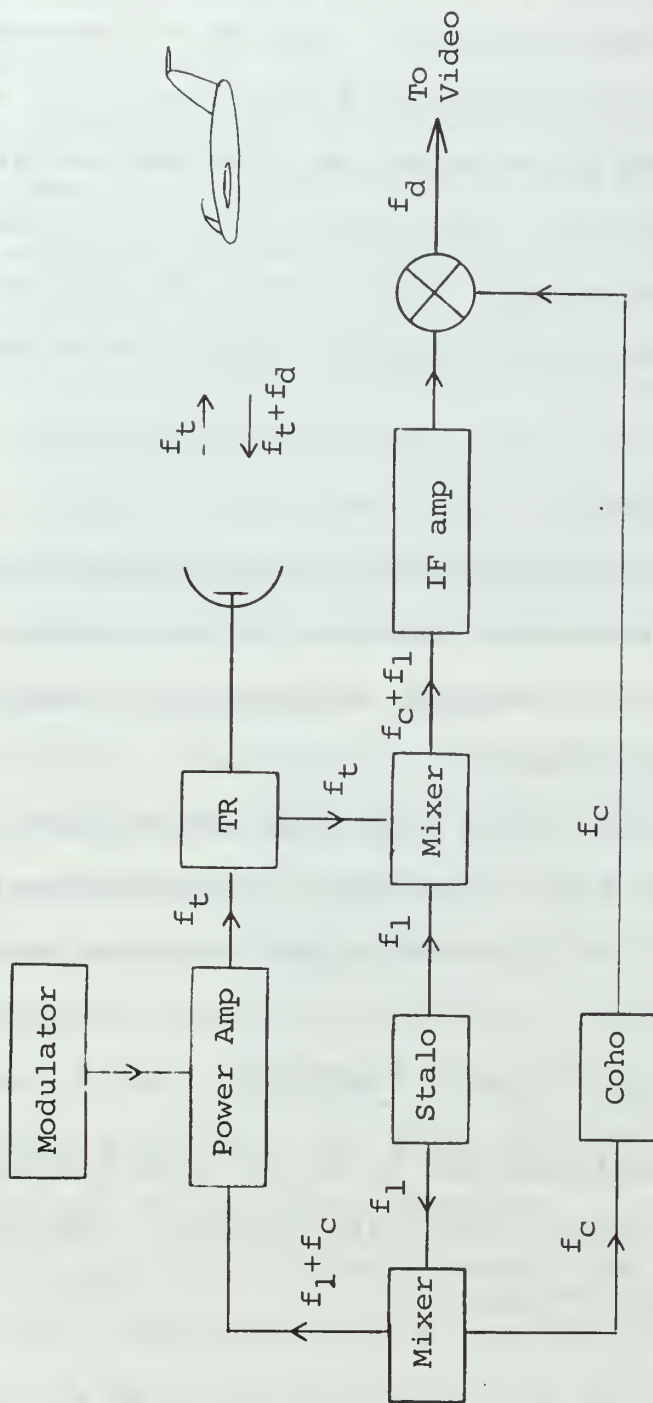


Figure 4.16. MTI radar.

where

$A_2$  = the amplitude of the echo signal

$f_t = f_c + f_1$  = the carrier frequency

$f_1$  = the stable local oscillator, or stalo frequency

$f_d$  = doppler frequency shift

$R_o$  = range of the target producing the echo

$c$  = velocity of propagation

The target echo signal and the stalo output are heterodyned in the mixer stage of the receiver. The difference frequency component from the mixer is retained and is a voltage given by

$$V_{\text{diff}} = A_3 \sin \left[ 2\pi (f_c + f_d)t - 4\pi f_t R_o / c \right].$$

After being amplified in the IF amplifier, this signal is mixed with the reference signal in the phase detector. The phase-detector output is given by

$$V_{\phi} = A_4 \sin \left[ 2\pi f_d t - 4\pi f_t R_o / c \right]$$

For stationary targets  $f_d$  will be zero, hence  $V_{\phi}$  will not vary with time and can assume any constant value from  $-A_4$  to  $+A_4$ , including zero. However, if the target does have a radial velocity component with respect to the radar,  $f_d$  is not zero and the phase-detector output will be a function of time. On successive A-scope sweeps, echoes from fixed targets will remain constant, whereas echoes from moving targets will vary in amplitude from sweep to sweep producing

the so-called "butterfly" effect on the A-scope. This is illustrated in Figure 4.17. For PPI presentation the dc component of fixed targets can be filtered out by the use of a delay-line canceler.

The characteristic feature of coherent MTI is that the transmitted signal must be coherent (in phase) with the reference signal in the phase detector. This requirement is easily met in the complementary-series pulse-compression system of Figure 4.3, in fact the complementary-series pulse-compression radar is automatically an MTI device since phase detection is an inherent requirement for matched-filter reception of phase-modulated waveforms. Thus nothing need be added. As has already been noted, if MTI is not desired, the received pulse could be quadrature phase detected.

Pulse-compression systems have an exclusive advantage over short-pulse systems as concerns MTI. Figure 4.18 shows the video pulse trains for targets of two different velocities. If  $f_d > 1/\gamma$ , the frequency of the video pulses is high and it is possible to obtain doppler information from only one received pulse. In this case no ambiguities in the measurement of doppler frequency can occur. If, however, the doppler frequency is less than  $1/\gamma$  the video pulse train appears as in Figure 4.18c, and many pulses will be needed to extract the doppler information.

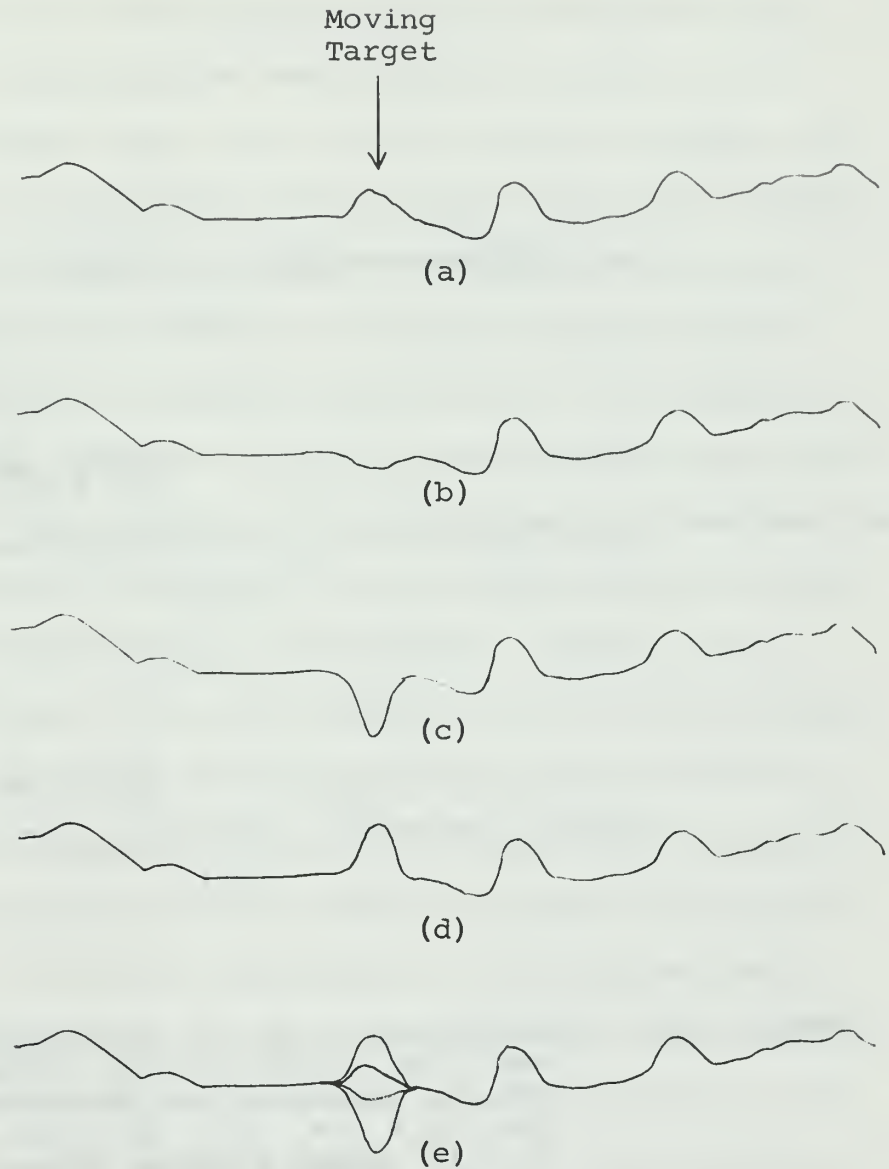


Figure 4.17. Successive A-scope sweeps for the MTI radar shown in Figure 4.14. Figure 4.16e represents the sum of Figures 4.16a to 4.16d. The moving target echo varies from sweep to sweep. (After Skolnik, Radar Systems, McGraw-Hill, New York: 1962)

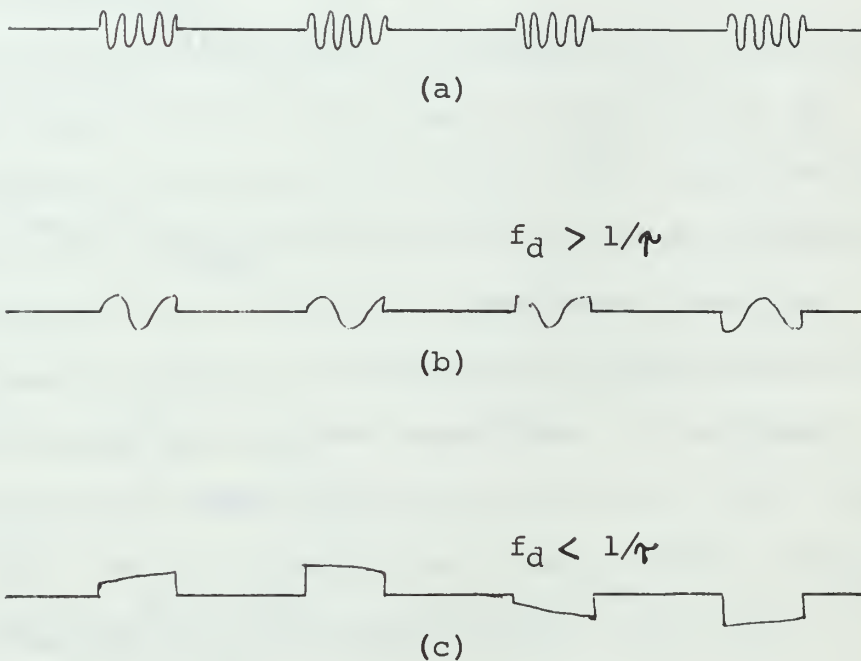


Figure 4.18. The waveform in (a) is the output of the IF amplifier in Figure 4.14. Waveforms (b) and (c) represent the phase-detector output for  $f_d > 1/\tau$  and  $f_d < 1/\tau$ . (After Skolnik, Radar Systems, McGraw-Hill, New York; 1962)

Ambiguities in the measurement of doppler frequency can occur in the discontinuous measurement of Figure 4.18c.

For an S-band radar with a pulse duration of one microsecond, which is characteristic of many short-pulse radars, the doppler frequency would have to be greater than one Mhz, corresponding to a target velocity greater than  $10^5$  meters per second for doppler information to be obtained in a single pulse. Targets ordinarily encountered travel much slower than this; therefore for most targets of interest the video pulse will look like 4.18c, and many pulses will be required to obtain doppler information. However, with pulse-compression, the pulse duration can be lengthened by a factor of 10 to 100 without degrading range resolution, resulting in a dramatic reduction of both doppler ambiguities and the amount of time needed to extract the doppler information. It can be shown that in the doppler domain, the zero crossings of the ambiguity function move closer to the origin of the range-doppler axis as the length of the code is increased, assuming that  $\tau'$ , the time duration of a subpulse, is constant.

The next chapter contains a summary of the advantages of complementary-series pulse-compression radar and the conclusions reached as a result of the work described in this chapter. Several suggestions for further research are also presented.

## V. CONCLUSIONS

### A. SUMMARY

The work presented in this thesis had as its objective a study of the feasibility of using complementary series as a method of pulse compression. Instrumentation of an entire radar system was beyond the scope of the master's thesis, therefore only the generation of the transmitted pulse waveform and its matched-filter reception were studied. Even this reduced objective would prove an extremely complicated task if long complementary codes were used; therefore a code of length four was chosen.

Delay lines were found to be one acceptable method of forming the transmitted pulse waveforms. A bank of gated amplifiers was also used with success.

Several methods of autocorrelation of received pulses were studied, including that of using the same delay line for autocorrelation as was used for generation of the transmitted waveform, but with the received pulse entering the delay line from the opposite end. Of these various methods, the most successful was to phase-detect the received pulses before autocorrelating them. In addition, in the case of moving targets it would be necessary to amplitude-detect the waveform representing the sum of the two individual autocorrelation functions.

The advantages of any pulse-compression radar, as compared to a short-pulse radar can be summarized by the following list:

1. Maximum range may be increased since the pulse energy is a linear function of the pulse duration, which may be increased by a factor of 10 to 100. This allows more efficient use of transmitter power (longer duty cycle).
2. Better range resolution due to compression of the long pulse in the receiver.
3. Reduction of doppler ambiguities and the time required to obtain doppler information.
4. Increased enemy difficulty in detecting the wideband, noiselike transmitted signal.
5. Excellent anti-jamming characteristics.
6. Receiver signal-to-noise ratio is maximized by the use of the matched filter.

Complementary-series pulse-compression radar offers the additional refinement that the ambiguities are minimized and the range ambiguities are completely eliminated at zero doppler. It suffers the disadvantage that both sequences must be transmitted.

The four-element sequences used in the system described in Chapter IV would not provide a significant improvement in range and doppler resolution. Longer codes are available but of course the implementation of these would be more complex.

#### B. AREAS OF POTENTIAL STUDY

An obvious possibility for further work on complementary-series pulse compression is to use the pulse-modulating and



autocorrelating circuitry, developed as a result of work on this thesis, on a coherent radar. It would be interesting to compare the radar's performance with and without the pulse compression. A means of transmitting both sequences simultaneously would have to be developed.

A second suggestion is to investigate the quadrature phase detection for non-MTI use.

## APPENDIX A

### DELAY-LINE CHARACTERISTICS

Lumped-parameter delay lines, consisting of LC T-sections, were chosen to be used in this project for several reasons. The components, inductors and capacitors, were readily available. These delay lines could be built in compact form, as opposed to the great length of coaxial cable that would have been required to do the same job. In addition, the lumped-parameter lines could be built with very small attenuation, and they could be easily tapped.

The major design parameters are the characteristic impedance  $Z_0$ , the cutoff frequency  $f_{CO}$  and the delay per section,  $T_S$ . These parameters are given in terms of  $L_S$  and  $C_S$  by the following relations:

$$Z_0 = (L_S/C_S)^{1/2}$$

$$T_S = (L_S C_S)^{1/2}$$

$$f_{CO} = 1/\sqrt{L_S C_S}$$

where  $L_S$  and  $C_S$  are the inductance and capacitance per section, respectively. The physical layout of the lines is as shown in Figure A.1.

The characteristic impedance was chosen as 50 ohms, as most of the laboratory signal generators have a source impedance of this value and any reflections at the source would be minimized. A second reason is that tapping of the

delay line would introduce reflections at the tap because of the loading effect unless the line sees a high impedance at the tap compared to its own characteristic impedance, and this requirement is met more easily if the line's characteristic impedance is low.

It was desirable to make  $f_{CO}$  several times as large as the carrier frequency, as artificial lines are dispersive near the cutoff frequency. In addition, it was necessary to consider component sizes in the light of what was on hand in supply in sufficient quantities.

The choice of  $L_S = 2$  microhenries and  $C_S = 800$  picofarads met the above requirements and gave a cutoff frequency of 7.95 Mhz and a  $T_S$  of 0.04 microseconds. The choice of a 2-Mhz carrier, a four-digit code, and four complete cycles of carrier in each subpulse dictated a requirement of 300 LC sections, a number which was not considered unmanageable.

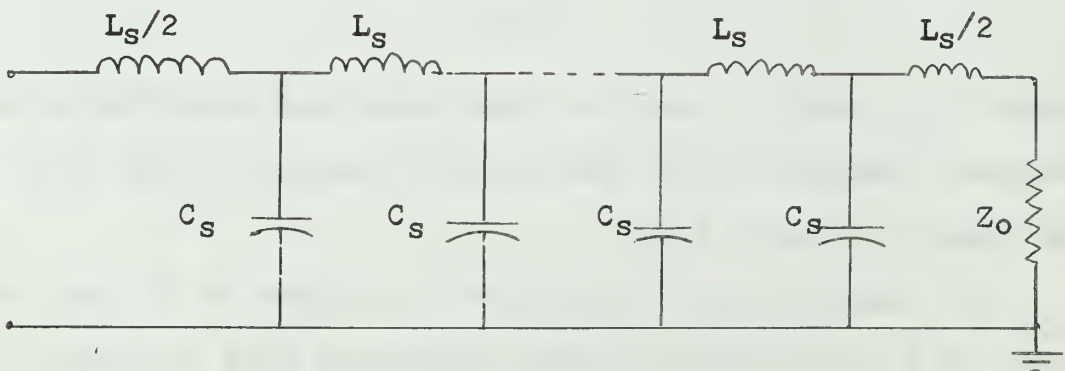


Figure A.1. Lumped-parameter delay line.

The inductors were wound on one-half-inch plastic tubular forms using 20-gauge varnished copper wire, and were 14 turns each. They were arranged on the lines with axes of adjacent coils perpendicular in order to minimize mutual coupling. Capacitors of extremely tight tolerance were not available, so each capacitor was trimmed with a smaller capacitor to  $800 \pm 3$  pf using an impedance bridge.

The resulting delay line showed very little loss and the delay and characteristic impedance were very close to those given by the equations above, even though those equations are for lossless artificial lines.

APPENDIX B

TRANSMIT-RECEIVE SWITCH,  
AS USED IN FIGURE 4.3

This switch, shown in Figures 4.3 and 4.4, is normally in the receive position, but switches to the transmit position during transmission. It was constructed using two FETs which were biased on and off by pulses triggered by the gated amplifier of Appendix G. The circuit was as shown in Figure B.1

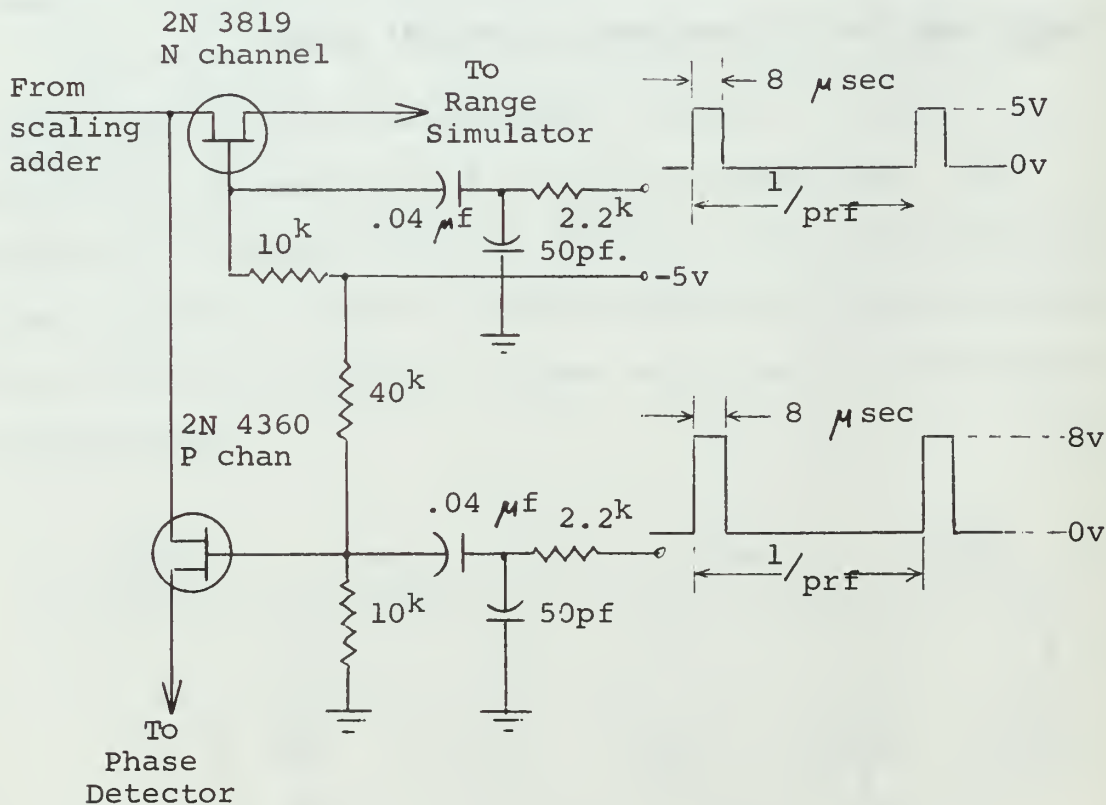


Figure B.1. Transmit-receive switch.

## APPENDIX C

### SCALING ADDERS

The five scaling adders required for the project were built using RCA CA-3029A operational amplifiers using a bias and phase-compensation circuit as shown in Figure C.1. The input pot settings are typical but varied from adder to adder.

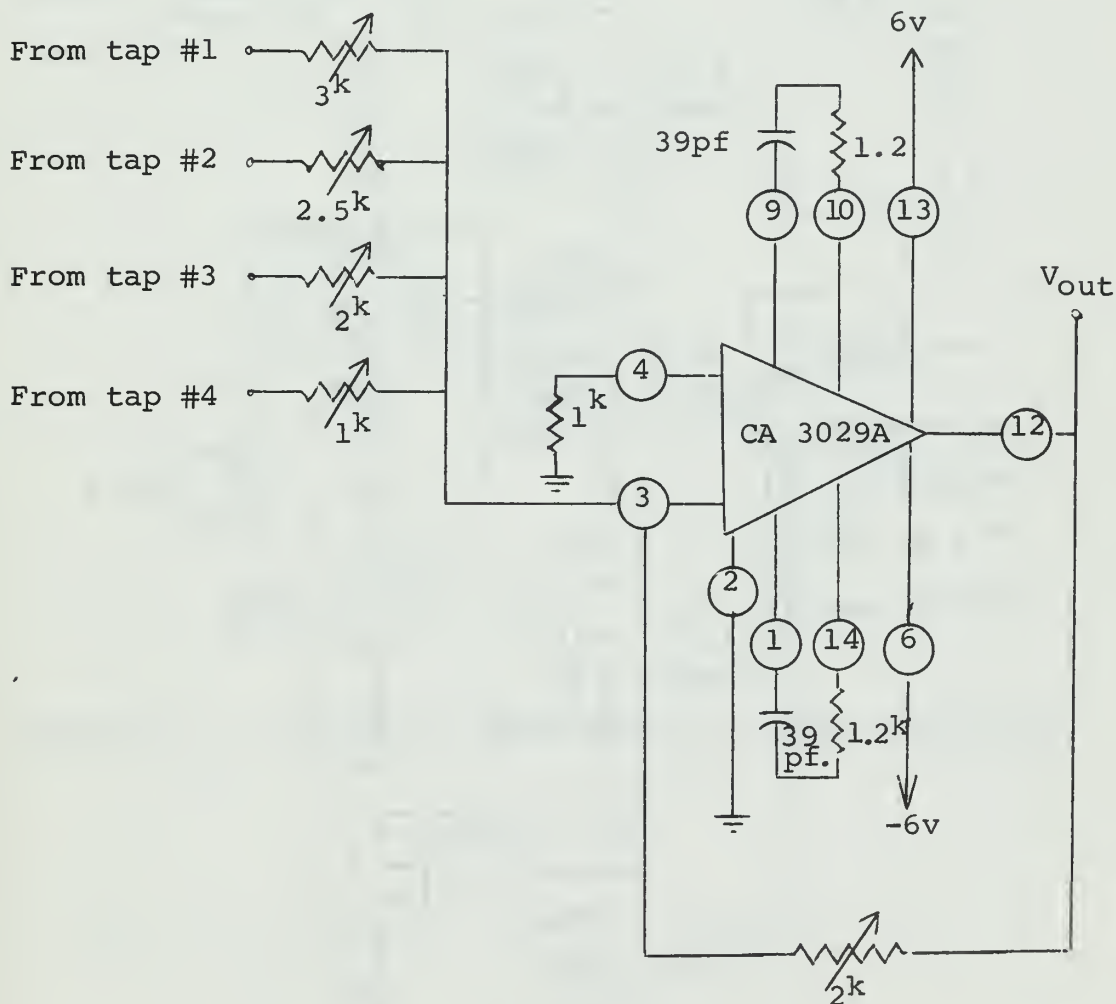


Figure C.1. RCA CA-3029A operational amplifier used as a scaling adder.

APPENDIX D

CIRCUIT DIAGRAM OF MODULATOR  
USED TO REPLACE THE DELAY LINE FOR  
GENERATING THE TRANSMITTED PHASE-CODED PULSE

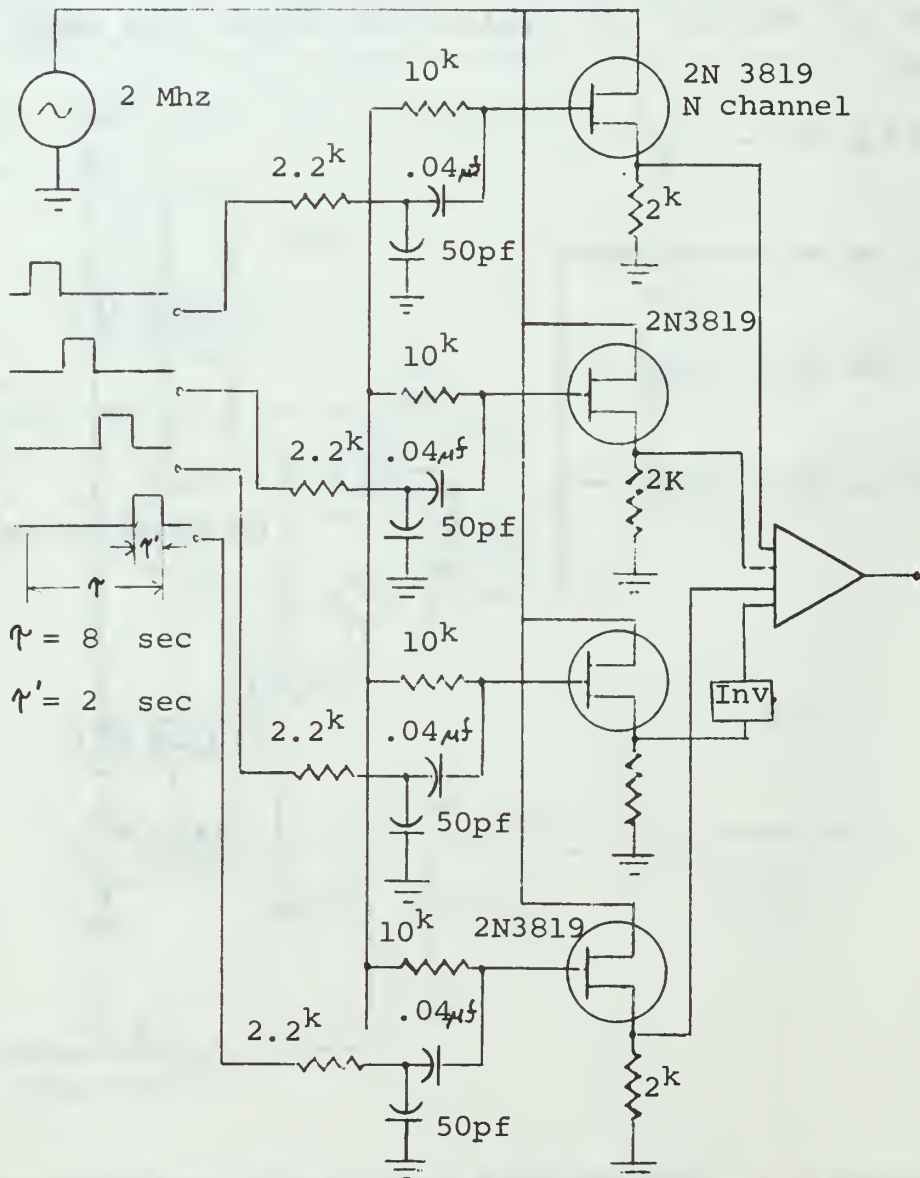


Figure D.1. Modulator for generating the transmitted waveform.

APPENDIX E  
BUFFING AMPLIFIERS

Buffing amplifiers are shown at various points in the various block diagrams of Chapter IV. These consisted of Darlington pairs, using 2N3705 silicon NPN transistors, as shown in Figure E.1.

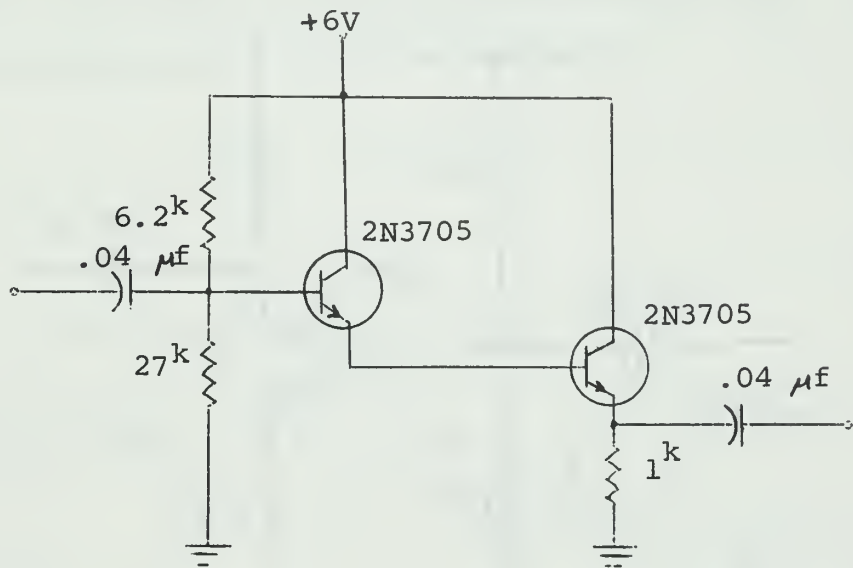


Figure E.1. Darlington pair used as a buffer amplifier.



## APPENDIX H

### RELCOM PHASE-DETECTORS

The phase-detector used was the Relcom Model M1, which is a broadband ring modulator employing hot-carrier diodes and designed for use in a 50-ohm system. The phase-detector output versus phase difference graph was shown in Figure 4.14. The circuit diagram of the mixer is shown in Figure H.1.

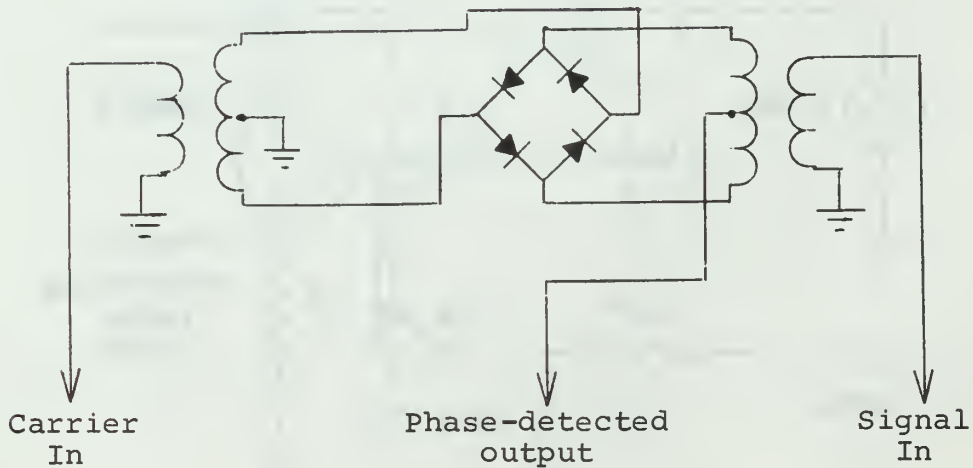


Figure H.1. Schematic of the Relcom M1 phase detector.

## REFERENCES

1. Woodward, P. M., Probability and Information Theory With Applications to Radar, New York: McGraw-Hill, 1953.
2. Cook, C. E., and Bernfeld, Marvin, Radar Signals, New York: Academic Press, 1967.
3. Klauder, J. R., Price, A. C., Darlington, S., and Albersheim, W. J., "The Theory and Design of Chirp Radars," Bell Systems Technical Journal, Vol. 39, pp. 745-808, July 1960.
4. Elspas, B., "A Radar System Based on Statistical Estimation and Resolution Considerations," App. Elect. Lab. Stanford University Tech. Rpt. 361-1, August 1955.
5. Pettit, R. H., "Pulse Sequences With Good Autocorrelation Properties," Microwave Journal, Vol. 10-3, pp. 63-67, February 1967.
6. Huffman, D. A., "The Generation of Impulse-Equivalent Pulse Trains," IRE Trans.-IT, Vol. IT-11, No. 4, pp. 533-537, October 1965.
7. Frank, R. L., "Polyphase Codes with Good Nonperiodic Correlation Properties," IEEE Trans.-IT, pp. 43-45, January 1963.
8. Yamagishi, F., and Hasegawa, T., "On the Auto-correlation Pulse Compressed Radar System," Memoirs of the Defense Academy, Japan, Vol. VII, No. 2, pp. 411-450, 1967.
9. Golomb, S. W., and Scholtz, R. A., "Generalized Barker Sequences," IEEE Trans.-IT, Vol. IT-11, No. 4, pp. 533-537, October 1965.
10. Golay, M. J. E., "Complementary Series," IRE Trans.-IT, pp. 82-87, April 1961.
11. Akita, R. M., An Investigation of the Narrow-band and Wideband Ambiguity Functions for Complementary Codes, M.S. Thesis, Naval Postgraduate School, Monterey, California, June 1968.
12. Jauregui, S., A Theoretical Study of Complementary Binary Code Sequences and a Computer Search for New Kernels, PhD Dissertation, Naval Postgraduate School, Monterey, California, May 1962.

13. Skolnik, M. I., Radar Systems, New York: McGraw-Hill, 1962.

INITIAL DISTRIBUTION LIST

	No. Copies
1. Defense Documentation Center Cameron Station Alexandria, Virginia 22314	20
2. Library Naval Postgraduate School Monterey, California 93940	2
3. Commander Navships Systems Command (Code 004G) Department of the Navy Washington, D. C. 20360	1
4. Professor D. B. Hoisington (Thesis Advisor) Department of Electrical Engineering Naval Postgraduate School Monterey, California 93940	1
5. LT G. J. Sieren Manned Space Station Design Management Team National Aeronautics and Space Administration Marshall Space Flight Center Huntsville, Alabama 35812	2



## DOCUMENT CONTROL DATA - R &amp; D

(Security classification of title, body of abstract and indexing annotation must be entered when the overall report is classified)

1. ORIGINATING ACTIVITY (Corporate author) Naval Postgraduate School Monterey, California 93940		2a. REPORT SECURITY CLASSIFICATION Unclassified	
		2b. GROUP	
3. REPORT TITLE A Study of Radar Pulse Compression Using Complementary Series to Modulate the Transmitted Waveform			
4. DESCRIPTIVE NOTES (Type of report and, inclusive dates) Master's Thesis		December 1969	
5. AUTHOR(S) (First name, middle initial, last name)			
6. REPORT DATE December 1969		7a. TOTAL NO. OF PAGES 75	7b. NO. OF REFS 13
8a. CONTRACT OR GRANT NO.		9a. ORIGINATOR'S REPORT NUMBER(S)	
b. PROJECT NO.			
c.		9b. OTHER REPORT NO(S) (Any other numbers that may be assigned this report)	
d.			
10. DISTRIBUTION STATEMENT This document has been approved for public release and sale; its distribution is unlimited.			
11. SUPPLEMENTARY NOTES		12. SPONSORING MILITARY ACTIVITY Naval Postgraduate School Monterey, California 93940	
13. ABSTRACT Pulse compression radars have resulted from the need to put more energy into a transmitted pulse by increasing the pulse duration, yet retaining or improving the target range resolution. FM chirp and phase-coded pulse compression using a single binary code to modulate the carrier are somewhat degraded by the amount of hash, or range sidelobes in the output of the matched-filter receiver.  Pulse compression using complementary series, in which two binary series are transmitted, results in no range sidelobes in the detected pulse, since the autocorrelation functions of the two series completely cancel each other everywhere except at zero shift, where they add to produce a sharp peak with amplitude 2N times the received pulse amplitude, where N is the number of digits in each series.  After introductory material on complementary series and pulse-compression systems, this thesis discusses the design, construction and testing of a pulse-compression system using complementary series of length four. The intent was to show feasibility, rather than to produce results using actual targets.			

14.

KEY WORDS

LINK A

LINK B

LINK C

ROLE

WT

ROLE

WT

ROLE

WT

AUTOCORRELATION

COMPLEMENTARY SERIES

MATCHED FILTER

PULSE COMPRESSION

RADAR

RANGE SIDELOBES













thes4935

A study of radar pulse compression using



3 2768 000 99087 3  
DUDLEY KNOX LIBRARY